JOURNAL OF GEOPHYSICAL RESEARCH, VOL. 95, NO. B11, PAGES 17,475–17,502, OCTOBER 10, 1990

Evolution of the Walvis Ridge-Rio Grande Rise Hot Spot System: Implications for African and South American Plate Motions Over Plumes

JOHN M. O'CONNOR AND ROBERT A. DUNCAN

College of Oceanography, Oregon State University, Corvallis

Crystallization ages of volcanic rocks, dredged or drilled from the Walvis Ridge (ten sites) and the Rio Grande Rise (one site), have been determined by the $^{40}Ar/^{39}Ar$ incremental heating technique. The fundamentally age-progressive distribution of these basement ages suggests a common hot spot source for volcanism on the island of Tristan da Cunha, along the Walvis Ridge and Rio Grande Rise, and for the formation of the continental flood basalts located in Namibia (Africa) and Brazil (South America). The Walvis Ridge–Rio Grande Rise volcanic system evolved along a section of the South Atlantic spreading-axis, as the African and South American plates migrated apart, astride, or in close proximity to, an upwelling plume. Reconstructions of the spatial relationship between the spreading-axis, the Tristan hot spot, and the evolving Walvis Ridge–Rio Grande Rise volcanic feature show that, at about 70 Ma, the spreading-axis began to migrate westward, away from the hot spot. The resulting transition to intraplate hot spot volcanism along the Walvis Ridge (and associated termination of Rio Grande Rise formation) also involved a northward migration of previously formed African seafloor over the hot spot. Rotation parameters for African motion over fixed hot spots (i.e., absolute motion) have been recalculated such that the predicted trail of the Tristan hot spot agrees with the distribution of radiometric and fossil basement ages along the Walvis Ridge. African absolute motion has been extended to the South and North American plates, by the addition of relative motion reconstruction poles.

Introduction

Apart from the mid-Atlantic spreading-axis, the Walvis Ridge (Figure 1*a*) and Rio Grande Rise (Figure 1*b*) are the two most prominent bathymetric features in the South Atlantic basin. Broadly speaking, the Walvis Ridge and the Rio Grande Rise form a V-shaped pair of volcanic lineaments, whose axis of symmetry is the South Atlantic spreading-center (Figure 2). *Morgan* [1971, 1972], following *Wilson* [1963], related the formation of these volcanic trails to hot spot volcanism, presently active beneath the ocean island of Tristan da Cunha.

The Walvis Ridge can be subdivided into three morphologically distinct regions, two of which appear to have a comparable or "mirror image" region on the Rio Grande Rise. The broad eastern plateau of the Walvis Ridge projects seaward from the African coast to about 5°E. This plateau initially evolved in conjunction with the Torres Arch, later with the broad plateau of the Rio Grande Rise, and finally with the northeastern shoulder of the Rio Grande Rise. The central section of the Walvis Ridge (about 5°E to 2°W) includes three distinct, subparallel NE-trending ridges, which formed in conjunction with the eastern, N-S ridge of the Rio Grande Rise. Finally, the Walvis Ridge merges into a line of large seamounts, which extends southwestward from the central section of the Walvis Ridge toward Tristan da Cunha. A corresponding seamount chain does not appear to exist on the South American plate; however, the Zapiola Seamount Complex, located to the south of the Rio Grande Rise may be related in some way to the Tristan hot spot.

The island of Tristan da Cunha is located ~550 km to the east of the present day spreading-axis, on C6 oceanic crust (19 Ma after the time scale of *Kent and Gradstein* [1986], used throughout this discussion). Apparent K-Ar ages ranging from 0.01 ± 0.02 Ma to 0.21 ± 0.01 Ma have been determined for this island [*McDougall and Ollier*, 1982], with the most recent volcanic eruption having occurred in 1962 [*Barker*, 1964].

This paper reports the results of sixteen ^{40}Ar-^{39}Ar incremental heating studies of volcanic rocks recovered from ten locations distributed along the Walvis Ridge and a single sample site located on the Rio Grande Rise (Figure 2). The changing spatial relationship between the spreading-axis, the Tristan hot spot, and the evolving structure of the Walvis Ridge–Rio Grande Rise system, has been reconstructed for selected times. These reconstructions provide new insights into the influence of hot spot and spreading-axis interactions on the structural and compositional evolution of the Walvis Ridge–Rio Grande Rise volcanic system. Previously estimated finite reconstruction poles for African plate motion over hot spots (i.e., absolute motion) have been adjusted such that the predicted track of the Tristan hot spot on the African plate reconstructs the distribution of the new Walvis Ridge basement ages. The absolute motions of the South and North American plates have, in turn, been calculated by the addition of appropriate relative motion reconstruction poles.

Geological Setting

The Parana (southeast Brazil) and the Etendeka (southwest Africa) continental flood basalts (Figure 2) represent the earliest known manifestation of the hot spot responsible for forming the Walvis Ridge–Rio Grande Rise. These flood basalt fields are shown to have formed as adjoining neighbors, on reconstruction of the South Atlantic for early Cretaceous time [*Rabinowitz and LaBrecque*, 1979] and Figure 9*a*. Geochemical and isotopic data support a common source for the Parana–Etendeka and Walvis Ridge basalts [*Hawkesworth et al.*, 1986]. K-Ar ages ranging from 114 to 196 Ma have been reported for the Etendeka lavas [*Siedner and Miller*, 1968; *Siedner and Mitchell*, 1976]. *Erlank et al.* [1984] have recognized three petrographic units within these basaltic lavas: the coastal Albin type, the widespread and voluminous Tafelberg type, and in the faulted coastal zone, late stage cross-cutting dolerite dikes which have been grouped as the Horingbaai type. K-Ar ages for these three units range from 88 to

Copyright 1990 by the American Geophysical Union.

Paper number 90JB00782.
0148-0227/90/90JB-00782$5.00

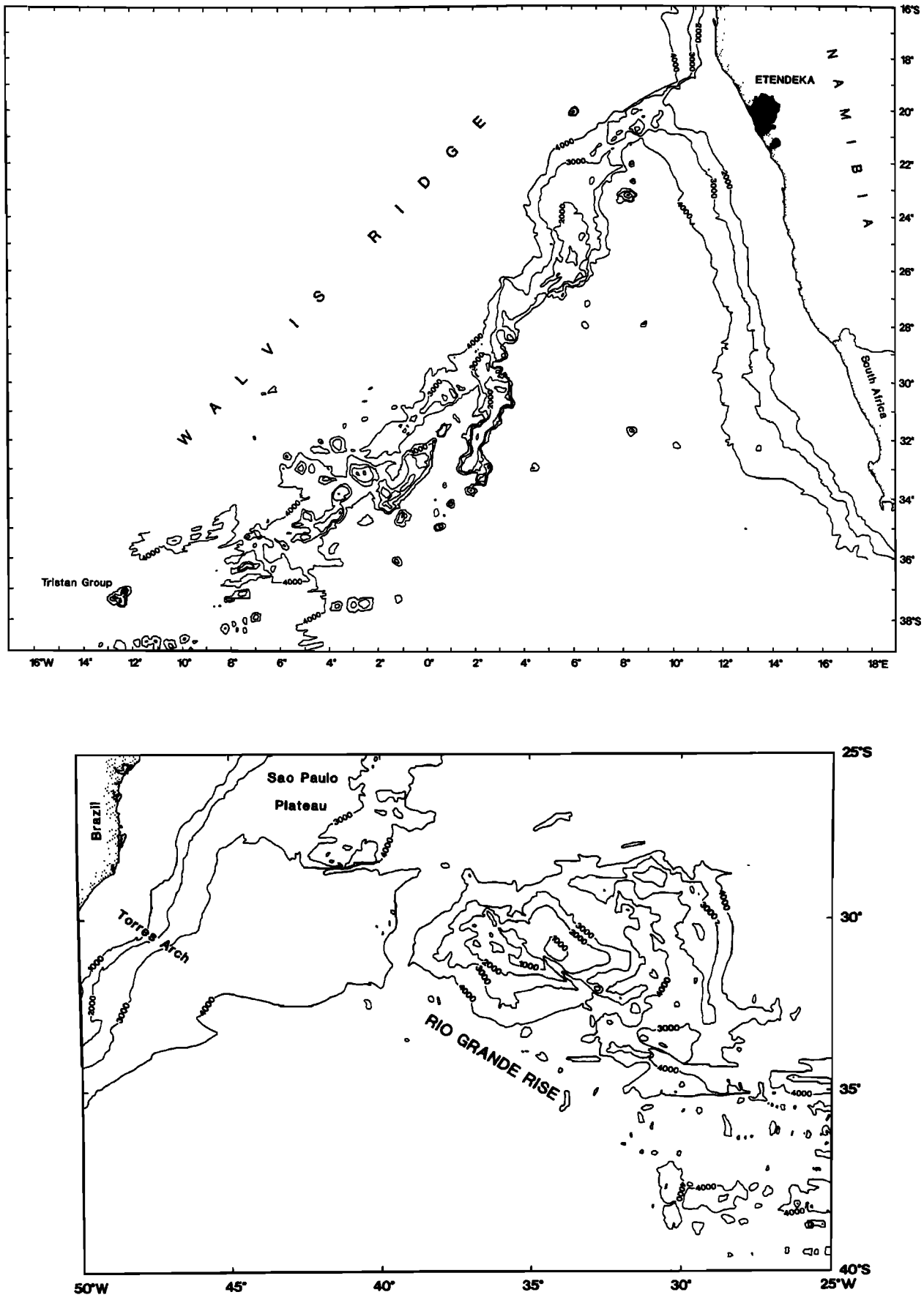

Fig. 1. (*a*) Bathymetry for the Walvis Ridge, contoured in 1000 m intervals [after *Needham et al.*, 1986]. (*b*) Bathymetry for the Rio Grande Rise, contoured in 1000 m intervals [after *Cherkis et al.*, 1989]. Mercator projections.

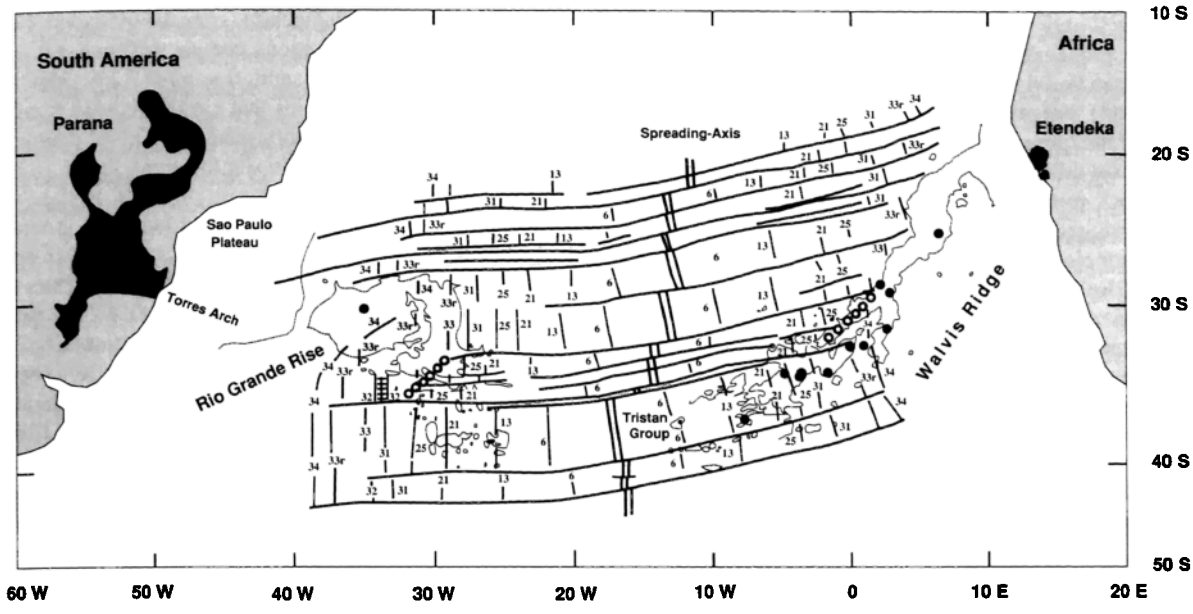

Fig. 2. Solid circles show the locations of the sample sites from which the rocks analyzed in this study were recovered. Seafloor spreading anomalies and fracture zones are from *Cande et al.* [1989]. A fossil spreading center south of the Rio Grande Rise is shown by a "railroad track". The location to which the spreading-axis jumped, between C32 and C30 times, is shown as a line of open circles on both the Rio Grande Rise and the Walvis Ridge. Mercator projection.

377 Ma. The authors attribute these anomalously high K-Ar ages (as indicated by stratigraphic relationships) to excess argon "inherited" at the time of crystallization. Feldspar separates taken from two fresh Horingbaai dolerites yielded fairly convincing ^{40}Ar-^{39}Ar plateau ages of 125, and 125 to 130 Ma [*Erlank et al.*, 1984]. These late stage intrusives may represent a final upwelling of continental hot spot volcanism immediately preceding the initiation of Walvis Ridge construction. In Brazil, Parana volcanism also appears to have peaked at between 120 and 130 Ma [*Amaral et al.*, 1966; *McDougall and Ruegg*, 1966; *Melfi*, 1967; *Siedner and Mitchell*, 1976; *Cordani et al.*, 1980].

Based on the results of seismic reflection profiling, *Austin and Uchupi* [1982] have suggested that the South Atlantic began to open in the form of a northward propagating rift. The oldest seafloor spreading anomaly identified in the South Atlantic at the latitude of Capetown is M11 (133 Ma), while the oldest anomaly recognized off of the Namibian coast is M4 (126 Ma) [*Cande et al.*, 1989]. As the Etendeka and Parana flood basalts appear to have erupted at about the same time that the northward-propagating South Atlantic rift reached the latitude of Namibia, a close association may have existed between hot spot volcanism and continental rifting. However, due to uncertainty in locating the continent-ocean boundary [e.g. *Rabinowitz*, 1976, 1978; *Scrutton*, 1978], it is presently difficult to determine whether or not, on reconstruction of the African and South American plates to a prerifting configuration, overlapping or misfit exists at the latitude of the Walvis Ridge–Rio Grande Rise. The existence of such an overlap would suggest that crustal stretching occurred in response to doming of the continental lithosphere by the upwelling plume, so supporting a relationship between rifting and hot spot volcanism. *Morgan* [1972], *Anderson* [1982] and *White and McKenzie* [1989] have suggested such a cause and effect relationship between Atlantic basin hot spots and the initiation of continental rifting.

The Walvis Ridge extends southwestwardly from the Etendeka flood basalts to about 10°E in the form of thinned continental crust, as shown by seismic reflection studies [*Sibuet et al.*, 1984]. This portion of the ridge is characterized by internal basement reflectors which dip to the west, while still further to the west (10°E to 8°E) the acoustic basement changes to that of typical oceanic crust [*Sibuet et al.*, 1984]. On the South American margin, the Parana lavas stretch seaward toward the Vema Channel in the form of the Torres Arch (Figure 1*b*) [*Kowsmann et al.*, 1977; *Kumar*, 1979].

The present day position of the spreading-axis in the latitudes of the Walvis Ridge and Rio Grande Rise is asymmetric with respect to the coasts of Africa and South America; i.e., the spreading-axis is located closer to the African than to the South American coast (Figure 2). The southern boundary of this spreading-axis asymmetry would appear to be the unnamed fracture zone located to the north of Tristan da Cunha (Figure 2). This asymmetry has been attributed to a succession of easterly and southeasterly spreading-axis migrations [*Mascle and Phillips*, 1972; *Sclater and McKenzie*, 1973; *Ladd*, 1974, 1976], which began prior to C34 (84 Ma) time. The first recorded eastward migration of the spreading-axis occurred to the north of the Walvis Ridge–Torres Arch lineament at early Albian–late Aptian time (97.5 to 115 Ma) [*Leyden et al.*, 1976; *Ponte and Asmus*, 1976; *Cande and Rabinowitz*, 1978, 1979; *Rabinowitz and LaBrecque*, 1979; *Kumar and Gamboa*, 1979]. The primary evidence for the timing of this axis jump is the asymmetric distribution of continental margin salt deposits, which are more extensive in the Brazilian compared with the Angolan basin. African plate Mesozoic magnetic anomalies located to the north of the Rio Grande Fracture Zone were transferred westward to the Sao Paulo plateau [*Cande and Rabinowitz*, 1978, 1979]; however, to the south of this fracture zone Mesozoic anomalies remained on the African plate [*Rabinowitz*, 1976]. The timing and location of the beginning of this second phase of spreading-axis migrations are not well constrained.

LaBrecque et al. [1984] mapped younger anomalies extending progressively southward and terminating against the northern

flank of the Walvis Ridge (Figure 2) and proposed that a southwardly propagating spreading-axis was involved in the formation of the Walvis Ridge–Rio Grande Rise volcanic system. *Barker* [1984] suggested that such easterly and southerly migrations of the spreading-axis represent a "recapturing process" of the westward drifting spreading-axis, by the Tristan da Cunha hot spot. Such spatial readjustments of the spreading-axis may therefore represent a process by which the axis maintained its position on, or close to, the Tristan hot spot for the duration of Rio Grande Rise formation.

Detrick and Watts [1979] and *Humphris and Thompson* [1983] have proposed that at about 80 Ma the mid-Atlantic axis began a westward migration away from the hot spot. The resulting transition to intraplate hot spot volcanism along the Walvis Ridge also involved a pronounced east-southeast ridge crest jump, sometime between anomaly 32 (71.4 Ma) and anomaly 30 (67 Ma) times, which has been mapped south of the Rio Grande Rise (Figure 2) [*Cande et al.*, 1988; after J. L. LaBrecque and J. M. Brozena, manuscript in preparation]. This ridge jump left a fossil spreading center roughly 200 km long, the location of which is consistent with a southward propagating rift model for spreading-axis involvement in the formation of the Walvis Ridge–Rio Grande Rise [*LaBrecque et al.*, 1984].

Sample Selection

The petrology and geochemistry of the Walvis Ridge and Rio Grande Rise samples selected for age determinations have been reported by *Humphris and Thompson* [1982, 1983], *Thompson and Humphris* [1984], and *Richardson et al.* [1982, 1984]. Overall, the Walvis Ridge and Rio Grande Rise samples range in composition from tholeiitic to alkalic basalts. These rocks generally contain phenocrysts of plagioclase feldspar up to 8 mm long and, less commonly, titaniferous augite in a groundmass composed of laths of plagioclase, granular pyroxene, Fe-oxides, and glass. Rock compositions contain between 1.0 and 4.8% MgO (dredged samples) and 0.9 and 7.2% MgO (drilled samples), representing liquids that are far evolved from primary melts. Brief sample descriptions and sample site coordinates are given in Table 1, with sample site locations shown in Figures 2 and 5.

Most of the rocks show patchy alteration of the groundmass to low-temperature Fe-oxides and clay minerals. This appears to have affected mainly the groundmass, but in some cases even the pyroxene microphenocrysts are replaced. Glass has devitrified, and very finely crystallized mesostasis (as much as 40% by volume of some samples) has altered in places to smectites and zeolites. This is further demonstrated by the moderately high total volatile contents (CO_2 plus H_2O^+), which range from 1.2 to 3.9%. Olivine is rarely present as a phenocryst phase or in the groundmass.

Much of the potassium in these rocks is likely to reside in the variably altered groundmass. The radiogenic ^{40}Ar ($^{40}Ar^*$) generated by the decay of ^{40}K at these sites (after crystallization) can be lost both by diffusion and the low-temperature formation of clay minerals, resulting in erroneously young conventional K-Ar ages [*Schlanger et al.*, 1984]. Smectites and zeolites crystallize from volcanic glass, infill vesicles and replace primary minerals.

Other complications encountered in applying the K-Ar technique to the dating of submarine volcanic rocks may arise from the fact that glassy submarine lavas may contain excess ^{40}Ar, due to the retention of mantle-derived Ar in magma erupted under high hydrostatic pressure [e.g., *Dalrymple and Moore*, 1968; *Dalrymple and Lanphere*, 1969; *Dymond*, 1970; *Aumento*, 1971]. Metasomatic addition of K, derived from seawater, to grain surfaces [*Melson and Thompson*, 1973; *Seidemann*, 1977] may lead to erroneously young K-Ar age determinations.

TABLE 1. Walvis Ridge and Rio Grande Rise Basalts Used for ^{40}Ar-^{39}Ar Age Determinations

Sample	Location (°S, °E)	Depth, m	Description
	Walvis Ridge		
AII-93-3-1	37° 05.7', -7' 46.7'	2600-2000	vesicular pl-basalt
AII-93-3-25	37° 05.7', -7° 46.7'	2600-2000	vesicular pl-basalt
AII-93-5-3	34° 17.3', -5° 01.5'	3100-3000	vesicular pl-basalt
AII-93-7-1	34° 30.1', -3° 37.6'	2200-2100	alkali pl-basalt
AII-93-8-11	34° 29.9', -3° 28.7'	2000-1500	alkali basalt
AII-93-10-11	34° 20.1', -1° 34.4'	2300-2000	basalt
AII-93-11-8	32° 58.2', -0° 01.1'	3100-1600	vesicular basalt
V29-9-1	32° 38.0', 1° 07.0'	3500	pl-basalt
AII-93-14-1	31° 59.6', 2° 23.6'	2300-1600	vesicular basalt
AII-93-14-19	31° 59.6', 2° 23.6'	2300-1600	aphyric basalt
AII-93-21-1	25° 26.1', 6° 42.2'	3200-2600	pl-basalt
DSDP 74-525-57-5, 104-106 -6, 41-43	29° 04.2', 2° 59.1'	3087	aphyric tholeiitic basalt
DSDP 74-528-40-5, 70-75	28° 31.5', 2° 19.4'	4280	phyric pl-basalt
DSDP 74-528-41-2, 40-42	28° 31.5', 2° 19.4'	4291	aphyric basalt
	Rio Grande Rise		
DSDP 72-516F-128-1, 22-24	30° 16.6', -35°17.1'	1268	phyric basalt
DSDP 72-516F-128-1, 104-107	30° 16.6', -35°17.1'	1268	phyric basalt

The available Walvis Ridge and Rio Grande Rise samples were examined in thin section in order assess the original igneous texture, crystallinity, and subsequent degree of alteration of the potassium-bearing phases. While no sample was regarded as being ideal for radiometric dating purposes, well-crystallized samples, displaying the lowest degrees of groundmass alteration, were selected for ^{40}Ar-^{39}Ar age incremental heating studies.

AGE MEASUREMENT METHODS

The ^{40}Ar-^{39}Ar method is based on the generation of ^{39}Ar from ^{39}K by the irradiation of K-bearing samples with neutrons in a nuclear reactor. The principles of this method of dating have been presented by *Dalrymple and Lanphere* [1971], *Dalrymple et al.* [1981*a*], and *McDougall and Harrison* [1988]. Samples selected for age studies were crushed after the removal of any obvious surface weathering and vesicle fillings. The 0.5 to 1.0 mm rock fragments were retained for dating experiments, ultrasonically washed in distilled H_2O, and dried. About one gram of each of the samples was encapsulated in an evacuated quartz vial and irradiated in the central thimble position of the U.S. Geological Survey TRIGA reactor for 15 hours at 1 MW power level, using the procedures described by *Dalrymple et al.* [1981*a*]. A hornblende flux monitor of known age (Mmhb-1), [*Samson and Alexander*, 1987] was irradiated with the basalts in order to determine the neutron flux density and the capture cross section of ^{39}Ar for neutrons during the irradiation, i.e., the efficiency of conversion of ^{39}K to ^{39}Ar expressed as the J-factor (Table 2).

Samples and standards were individually placed in an outgassed Mo crucible, which was then heated in a high-vacuum extraction line. The standards were fused in a single heating step, while the basalts were incrementally heated in a series of five steps (each of 30 min duration) and then melted during a sixth and final step. The isotopic composition of argon (^{40}Ar, ^{39}Ar, ^{37}Ar and ^{36}Ar) released from each individual heating or fusion step was measured immediately by means of an AEI MS-10S mass spectrometer, after active gases had been removed by cooling Ti-TiO_2 getters. The apparent ages of the individual heating steps were calculated from the measured $^{40}Ar^*$ to ^{39}Ar ratios, after corrections for all interfering nuclear reactions had been applied using the equation of *Brereton* [1970]. Hence an age-temperature spectrum was obtained for each sample, based on the $^{40}Ar^*/^{39}Ar$ compositions of the gas fractions released incrementally, from low to high temperature sites. Argon isotopic data and apparent ages are given in Table 2.

RESULTS

The most common age-temperature spectrum observed in this study consists of a middle temperature plateau bounded by higher ages at the low temperature steps, and conversely, by lower ages at the high temperature steps (e.g., Figure 3*e*). *Turner and Cadogan* [1974] first proposed that such an "inverse staircase" age-temperature profile might result from neutron-capture recoil of ^{39}Ar from K-rich to K-poor sites within fine-grained basalts, during irradiation. Because the low-temperature sites are K-rich, recoil effects may lead to the transfer of ^{39}Ar (but not $^{40}Ar^*$) from low temperature (i.e., alteration minerals and groundmass) to high-temperature sites (e.g., feldspar and pyroxene), resulting in a descending age-temperature release pattern. *Dalrymple and Clague* [1976], *Seidemann* [1978], and *McDougall and Duncan* [1988] have shown that significant amounts of ^{39}Ar may be lost from slightly altered volcanic rocks during the irradiation process. Thus, in conjunction with the loss of $^{40}Ar^*$ discussed earlier, ^{39}Ar may also be lost from, or relocated within, a multiphase sample.

Examination of apparent K/Ca ratios can be helpful in identifying the mineral phases that are contributing to different regions of the age spectrum [*Walker and McDougall*, 1982] (e.g., Figure 3*f*). With respect to the study reported here, low temperature steps generally correspond to high K/Ca phases, characteristic of K-rich alteration products such as smectite. The high apparent ages of these initial heating steps may reflect the loss or redistribution of ^{39}Ar due to neutron-induced recoil effects. The lower K/Ca values of the middle to high temperature steps are characteristic of unaltered, low K phases such as plagioclase. The plateau ages usually evident at these heating steps may be attributed to the diffusion of ^{40}Ar and ^{39}Ar from such unaltered phases. The highest temperature spectrum steps are commonly lower in age than that of the mid-temperature plateau and correspond to very low K/Ca ratios, which are characteristic of low K-phases, such as pyroxene. Recoil-induced addition of ^{39}Ar from low temperature high K-phases to K-poor high temperature phases, might account for such erroneously young ages in the age spectra.

Dalrymple et al. [1981*b*] suggested that, in cases where ^{39}Ar recoil is evident, the best age estimate for a sample comes from summing the gas composition of all the heating steps into a "recalculated" ^{40}Ar-^{39}Ar total fusion age. This calculation is based on the assumption that phases which lose ^{39}Ar during irradiation have also lost their $^{40}Ar^*$ over geological time. However, since ^{39}Ar recoil may be an incomplete process, a total fusion age which is not supported by both a clear plateau (particularly for the middle temperature steps) and a well constrained isochron age, must be interpreted cautiously. Other criteria, such as the consistency of ages for multiple samples from the same locality or independent geological constraints, can increase confidence in such total fusion ages.

Weighted mean plateau ages have been calculated for samples yielding an age-temperature plateau, primarily for middle temperature heating steps. These middle temperature sites are considered to be least disturbed by the loss or addition of ^{39}Ar resulting from recoil effects, as discussed above. The slope formed by the correlation of the $^{40}Ar/^{36}Ar$ and $^{39}Ar/^{36}Ar$ ratios for selected heating steps yielded an $^{40}Ar^*/^{39}Ar$ ratio, from which an isochron age was determined for most samples. Ideally, the $^{40}Ar/^{36}Ar$ intercept of such isochrons should reflect the composition of the rock at the time of crystallization, i.e., 295.5, consisting of only atmospheric argon without any contribution from potassium decay. Isochron slopes and intercepts were calculated using the least squares fitting technique of *York* [1969], which allows for correlated errors in both $^{40}Ar/^{36}Ar$ and $^{39}Ar/^{36}Ar$ isotopic ratios. Errors involved in measuring Ar ratios and J-factors (a typical error of 0.5% has been assigned) and in making corrections for interfering nuclear reactions were combined to yield a standard deviation for each heating age. The most reliable age-temperature spectrum and isochron plot for each sample site are shown in Figure 3. Plots of $^{36}Ar/^{40}Ar$ versus $^{39}Ar/^{40}Ar$ (inverse diagram) produced the same results as those estimated from isochron plots, as demonstrated by *Dalrymple et al.* [1988].

Samples AII-93-3-1 and AII-93-3-25 are from the same dredge haul and have very similar compositions [*Humphris and Thompson*, 1982]. Sample 3-1 produced a plateau age of 29.2 ±

TABLE 2*a*. Argon Isotopic Data for Walvis Ridge and Rio Grande Rise Whole Rock Samples

Increment	$^{40}Ar/^{36}Ar$	$^{40}Ar/^{39}Ar$	$^{37}Ar^*/^{40}Ar$	% Radiogenic ^{40}Ar	$\%^{39}Ar$ of Total	Age ± 1 σ x 10^{-6} years
			Sample AII-93-3-1, J = 0.00368			
1	339.8	65.520	0.0159	13.2	9.9	56.4 ± 2.2
2	404.0	19.140	0.0816	27.5	17.0	34.6 ± 0.5
3	952.8	6.278	0.4944	72.7	26.9	30.1 ± 0.2
4	1492.6	4.959	0.7498	85.9	25.2	28.4 ± 0.2
5	1076.2	4.120	0.9291	79.6	10.1	21.7 ± 0.3
6	340.0	2.948	7.3437	70.2	11.0	13.9 ± 0.5
			Sample AII-93-3-25, J = 0.00368			
1	322.7	61.240	0.0121	8.5	10.9	34.4 ± 3.4
2	356.7	29.520	0.0640	17.6	15.2	34.3 ± 0.8
3	669.0	7.763	0.4805	59.5	26.7	30.5 ± 0.3
4	1443.3	5.590	0.6147	84.2	26.6	31.3 ± 0.2
5	974.0	4.515	0.5951	74.2	9.5	22.1 ± 0.3
6	466.7	4.133	4.0620	68.2	11.2	18.8 ± 0.2
			Sample AII-93-5-3, J = 0.00368			
1	359.5	46.900	0.0230	18.0	2.4	55.1 ± 1.0
2	371.6	31.250	0.0250	20.7	7.9	42.4 ± 0.6
3	8211.2	6.060	0.2164	98.0	28.2	39.0 ± 0.6
4	3474.4	6.985	0.1503	92.6	26.7	42.5 ± 0.3
5	3397.8	6.259	0.1196	92.2	16.9	37.9 ± 0.3
6	17197.0	6.377	0.8137	89.1	17.9	37.5 ± 0.2
			Sample AII-93-7-1, J = 0.00368			
1	363.1	36.600	0.0200	18.7	13.0	45.0 ± 2.3
2	392.2	26.900	0.0449	25.0	15.2	44.0 ± 0.9
3	654.9	10.500	0.2036	56.4	18.2	39.0 ± 0.2
4	1926.0	6.501	0.6132	89.3	26.4	38.3 ± 0.2
5	1132.7	5.820	0.7350	79.5	18.1	30.5 ± 0.2
6	481.4	4.762	3.6127	66.7	9.1	21.2 ± 0.4
			Sample AII-93-8-11, J = 0.00368			
1	389.1	34.769	0.0348	24.3	19.1	55.3 ± 17.9
2	373.6	36.660	0.0522	21.3	12.0	51.2 ± 1.4
3	784.8	8.517	0.5394	66.5	24.0	37.3 ± 0.2
4	1148.2	6.722	0.8279	80.6	16.1	35.8 ± 0.4
5	732.9	5.313	1.0019	67.4	16.1	23.7 ± 0.1
6	537.7	4.565	2.5495	64.8	14.7	19.7 ± 0.3
			Sample AII-93-10-11, J = 0.00341			
1	509.9	24.890	0.0319	42.3	25.0	63.6 ± 0.4
2	571.4	18.420	0.0872	48.9	9.7	54.7 ± 0.3
3	561.2	18.000	0.1533	48.5	10.3	53.0 ± 0.4
4	529.2	16.830	0.2173	45.8	11.7	46.5 ± 0.4
5	513.0	16.800	0.2529	45.4	8.6	45.4 ± 0.6
6	475.0	18.390	0.4143	41.0	34.7	46.0 ± 0.3
			Sample AII-93-11-8, J = 0.00320			
1	1485.0	14.900	0.0158	80.2	13.4	67.5 ± 0.4
2	30782.6	11.290	0.0102	99.1	24.6	63.5 ± 0.8
3	58224.5	11.570	0.0108	99.6	28.3	65.3 ± 0.5
4	26671.7	11.400	0.0187	99.0	17.1	64.0 ± 0.4
5	13009.2	11.250	0.0579	98.1	11.7	62.6 ± 0.3
6	5467.1	11.260	0.0815	95.2	4.9	60.9 ± 0.3
			Sample V29-9-1, J = 0.00262			
1	340.3	105.300	0.0073	13.2	16.1	64.6 ± 1.4
2	337.9	81.740	0.0157	12.7	14.0	48.3 ± 2.0
3	371.5	53.580	0.0493	20.8	25.7	52.1 ± 0.5
4	380.3	45.100	0.0984	23.1	24.5	48.6 ± 0.5
5	302.1	181.400	0.0292	2.4	8.7	20.6 ± 1.3
6	292.4	151.870	0.1846	0.4	11.0	2.8 ± 1.7

TABLE 2*a*. (continued)

Increment	$^{40}Ar/^{36}Ar$	$^{40}Ar/^{39}Ar$	$^{37}Ar^*/^{40}Ar$	% Radiogenic ^{40}Ar	$\%^{39}Ar$ of Total	Age ± 1 σ x 10^{-6} years
			Sample AII-93-14-1, J = 0.00320			
1	602.8	23.460	0.0394	51.3	12.4	68.2 ± 0.4
2	10398.0	11.350	0.9980	97.9	14.6	63.1 ± 0.4
3	22614.3	11.030	0.0679	99.2	27.9	62.1 ± 0.3
4	28535.1	10.850	0.0037	99.2	20.9	61.1 ± 0.3
5	8278.9	10.490	0.0691	96.9	12.5	57.8 ± 0.3
6	3229.6	10.900	0.1022	91.6	11.8	56.8 ± 0.4
			Sample AII-93-14-19, J = 0.00368			
1	439.4	38.200	0.0135	32.8	10.3	81.5 ± 4.0
2	1183.0	13.910	0.0507	75.4	7.2	68.3 ± 0.4
3	7882.0	10.070	0.0891	96.9	27.7	63.6 ± 0.3
4	18683.4	9.495	0.0802	99.0	39.4	61.4 ± 0.3
5	3838.2	9.109	0.1050	93.1	8.4	55.4 ± 0.3
6	2549.5	8.255	0.6993	93.8	6.9	50.9 ± 0.5
			Sample DSDP 525A-57-5, J = 0.00341			
1	1795.1	15.790	0.1190	84.4	16.6	80.3 ± 0.5
2	5600.9	14.320	0.0900	95.4	14.5	82.2 ± 0.4
3	6807.2	13.606	0.1862	97.1	23.5	79.6 ± 0.4
4	4512.4	13.790	0.2129	95.1	21.0	79.0 ± 0.4
5	5178.7	13.300	0.1198	95.2	17.7	76.3 ± 0.4
6	1866.4	13.700	0.8566	90.8	6.6	75.3 ± 0.5
			Sample DSDP 528-40-5 (73-75), J = 0.00341			
1	419.4	45.380	0.0887	30.3	7.2	82.7 ± 0.5
2	869.8	19.970	0.2555	68.0	11.1	81.9 ± 0.4
3	883.5	18.130	0.4984	70.4	13.5	77.3 ± 0.4
4	641.3	22.590	0.3894	56.9	20.2	77.9 ± 0.4
5	1010.2	16.350	0.2826	72.9	26.4	72.1 ± 0.4
6	1365.9	13.320	1.3602	88.9	21.7	72.3 ± 0.4
			Sample DSDP 528-41-2 (40-42), J = 0.00341			
1	3212.4	10.953	0.0538	91.2	17.6	60.5 ± 0.3
2	9613.1	10.881	0.0785	97.5	13.6	64.1 ± 0.8
3	5510.4	11.645	0.0566	95.3	17.5	66.9 ± 0.5
4	915.4	17.902	0.0173	67.8	14.8	73.2 ± 0.4
5	6957.0	10.000	0.0373	95.9	21.5	58.1 ± 0.3
6	3308.4	9.555	0.2873	93.2	14.9	54.1 ± 0.3
			Sample AII-93-21-1, J = 0.002620			
1	440.7	55.310	0.0106	33.0	2.8	84.3 ± 0.7
2	480.4	52.740	0.0085	38.5	7.9	93.6 ± 0.8
3	467.9	59.250	0.0083	36.9	21.5	100.5 ± 1.1
4	484.7	40.550	0.0303	39.3	19.1	73.9 ± 3.5
5	848.2	19.800	0.2334	67.0	22.8	61.8 ± 0.3
6	445.6	23.583	0.2478	35.9	26.1	39.4 ± 0.3
			Sample DSDP 516F-128-1 (22-24), J = 0.002785			
1	509.5	51.590	0.0188	42.1	5.4	106.1 ± 1.8
2	581.9	40.100	0.0163	49.4	10.8	96.9 ± 0.6
3	761.0	32.500	0.0969	61.9	24.4	98.6 ± 0.6
4	1185.8	23.450	0.2542	77.0	22.8	88.9 ± 0.5
5	678.4	26.840	0.3936	59.5	17.9	79.1 ± 0.5
6	419.9	36.090	1.4133	40.6	18.6	74.7 ± 0.6
			Sample DSDP 516F-128-1 (104-107), J = 0.002785			
1	534.2	67.210	0.0198	44.8	15.1	145.5 ± 1.1
2	756.0	35.510	0.0760	61.5	22.8	106.7 ± 0.6
3	1377.4	22.130	0.2410	87.6	22.5	87.6 ± 0.4
4	1358.4	20.050	0.3920	81.3	14.7	80.5 ± 0.4
5	881.5	22.100	0.4537	70.0	10.8	76.5 ± 0.4
6	476.6	32.100	1.0919	40.8	14.1	66.1 ± 0.5

Here, $\lambda = 5.53 \times 10^{-10}$/year. Data in table have not been corrected for neutron interferences.
Correction factors: $(^{36}Ar/^{37}Ar)$ Ca = 0.000264; $(^{39}Ar/^{37}Ar)$ Ca = 0.000673; $(^{40}Ar/^{39}Ar)$ K = 0.0006.
* Corrected for decay since neutron irradiation ($\lambda\ ^{37}Ar = 1.975 \times 10^{-2}$/day).

TABLE 2*b*. Age Calculations From Argon Isotopic Data

	Plateau Calculation			Isochron Calculation			
Sample	Age (m.y.) ± 1σ	Steps Used	% of Total ^{39}Ar	Age (m.y.) ± 1σ	Steps Used	Intercept	Recalculated Total Fusion Age (m.y.) ± 1σ
AII-93-3-1	29.2 ± 0.2	2, 3, 4	69.1	28.4 ± 0.6	1, 2, 3, 4	317.4 ± 5.2	30.3 ± 0.3
AII-93-3-25	31.0 ± 0.2	1, 2, 3, 4	79.2	30.8 ± 0.4	1, 2, 3, 4	299.9 ± 3.6	29.5 ± 0.4
AII-93-5-3	38.7 ± 0.2	2, 3, 4, 5, 6	97.6	38.2 ± 1.1	1, 2, 3, 4, 5, 6	309.4 ± 9.2	40.1 ± 0.3
AII-93-7-1	38.5 ± 0.2	3, 4	44.6	38.0 ± 0.2	1, 2, 3, 4	307.6 ± 1.5	37.2 ± 0.4
AII-93-8-11	37.2 ± 0.2	1, 2, 3, 4	69.0	35.6 ± 0.3	1, 2, 3, 4	321.8 ± 4	37.5 ± 3.5
AII-93-10-11	46.2 ± 0.3	4, 5, 6	55.0	49.2 ± 5.5	4, 5, 6	280.9 ± 26	52.0 ± 0.3
AII-93-11-8	64.1 ± 0.3	2, 3, 4, 5	81.7	62.0 ± 1.3	1, 2, 3, 4, 5, 6	384.0 ± 44	64.4 ± 0.4
V29-9-1	50.3 ± 0.4	2, 3, 4	64.0	50.0 ± 7.1	2, 3, 4	295.6 ± 10.6	44.6 ± 0.5
AII-93-14-1	61.4 ± 0.3	2, 3, 4	63.4	60.2 ± 1.0	2, 3, 4	949.0 ± 556	61.6 ± 0.3
AII-93-14-19	61.5 ± 0.3	3, 4	67.0	59.9 ± 2.0	2, 3, 4, 5, 6	389.0 ± 90	63.4 ± 0.5
DSDP 525A-57-5, 104-106							
DSDP 525A-57-5, 41-43	79.4 ± 0.4	3, 4	62.3	82.0 ± 1.9	1, 2, 3, 4	288.0 ± 128	79.1 ± 0.4
DSDP 528-40-5 (73-75)	77.6 ± 0.5	3, 4	33.6	79.1 ± 6.3	1, 2, 3, 4	296.8 ± 45	75.9 ± 0.5
DSDP 528-41-2 (40-42)							62.5 ± 0.3
AII-93-21-1							69.8 ± 0.8
DSDP 516F-128-1 (22-24)				87.2 ± 8.9	1, 2, 3, 4, 5, 6	293.2 ± 41.9	88.7 ± 0.5
DSDP 516F-128-1 (104-107)							95.5 ± 0.5

0.2 Ma (69.1% of the total ^{39}Ar released), an isochron age of 28.4 ± 0.6 Ma (intercept of 317 ± 5.2), and a recalculated total fusion age of 30.3 ± 0.3 Ma. Sample 3-25 yielded a distinct middle temperature age plateau of 31.0 ± 0.2 Ma (79.2% of the total ^{39}Ar released) (Figure 3*a*) and an isochron age of 30.8 ± 0.4 Ma (intercept of 299.9 ± 3.6) (Figure 3*b*). The total fusion age is 29.5 ± 0.4 Ma. The best estimate of the apparent age of this site is considered to be between 30 and 31 Ma.

Sample AII-93-5-3 produced a plateau age of 38.7 ± 0.2 Ma (97.6% of the total ^{39}Ar released) (Figure 3*c*), an isochron age of 38.2 ± 1.1 Ma (intercept of 309 ± 9.2) (Figure 3*d*), and a recalculated total fusion age of 40.1 ± 0.3 Ma. The crystallization age at this site appears to be well constrained at between 39 and 40 Ma.

Samples AII-93-8-11 and AII-93-7-1 are from separate dredge hauls from the same volcano. Sample 8-11 yielded a middle temperature plateau age of 37.2 ± 0.2 (69% the total ^{39}Ar released), an isochron age of 35.6 ± 0.3 Ma (intercept of 322 ± 4.0), and a recalculated total fusion age of 37.5 ± 3.5 Ma. Sample 7-1 results show a middle temperature plateau age of 38.5 ± 0.2 Ma (45% of the total ^{39}Ar) (Figure 3*e*), an isochron age of 38.0 ± 0.2 Ma (intercept of 308 ± 1.5) (Figure 3*g*), and a recalculated total fusion age of 37.2 ± 0.4 Ma. The best estimate of the age of this volcano is between 38 and 39 Ma.

The crystallization ages of dredged samples AII-93-5, 7 and 8 (38 to 40 Ma) are supported by results from the nearby Deep Sea Drilling Project (DSDP) site 359, which encountered volcanic tuff dated radiometrically (K-Ar) at 40.3 ± 1.0 Ma [*Fodor et al.*, 1977].

Sample AII-93-10-11 showed evidence in its argon release pattern of ^{39}Ar recoil; however, we tentatively identify a questionable plateau age of 46.2 ± 0.3 Ma (the final 55% of the total ^{39}Ar released) (Figure 3*h*). An isochron age of 49.2 ± 5.5 Ma (intercept of 281 ± 26) has been calculated using the heating steps which were included in the plateau age calculation (Figure 3*i*). The proportion of radiogenic ^{40}Ar released during this experiment was low, not exceeding 50% for any of the six heating steps. The recalculated total fusion age of 52.0 ± 0.3 Ma provides a minimum estimate of the age of this sample site.

Sample AII-93-11-8 yielded a good plateau age of 64.1 ± 0.3 Ma (81.7% of the total ^{39}Ar released) (Figure 3*j*), a well-constrained isochron age of 62.0 ± 1.3 Ma (intercept of 384 ± 44) (Figure 3*k*), and a recalculated total fusion age of 64.4 ± 0.4 Ma. The apparent age of this sample site is 64 Ma.

Sample V29-9-1 results show a middle temperature plateau age of 50.3 ± 0.4 Ma (64% of the total ^{39}Ar released) (Figure 3*l*) and a somewhat poorly constrained isochron age of 50.0 ± 7.1 Ma (intercept of 296 ± 11) (Figure 3*m*). The recalculated total fusion age of 44.6 ± 0.5 Ma is significantly lower than the plateau age. The percentage radiogenic ^{40}Ar released during incremental heating was very low, reaching a maximum of 21%. The best estimate of the age of this sample is taken to be the 50.0 ± 0.4 Ma plateau age.

Samples AII-93-14-19 and AII-93-14-1 are from the same dredge haul. Sample 14-19 yielded a plateau age of 61.5 ± 0.3 Ma (67% of the total ^{39}Ar released), an isochron age of 59.9 ± 2.0 Ma (intercept of 389 ± 90), and a total fusion age of 63.4 ± 0.5 Ma. Sample 14-1 produced a reasonable plateau age of 61.4 ± 0.3 Ma (63.4% of the total ^{39}Ar released) (Figure 3*n*), an isochron age of 60.2 ± 1.0 Ma (intercept of 949 ± 556) (Figure 3*o*), and a total fusion age of 61.6 ± 0.3 Ma. The crystallization age of this site is between 61 and 62 Ma.

DSDP Transect of the Walvis Ridge

DSDP sites 525A, 528, and 527 constitute a SE-NW transect across the Walvis Ridge (Figure 2). The ages of drilled basalts

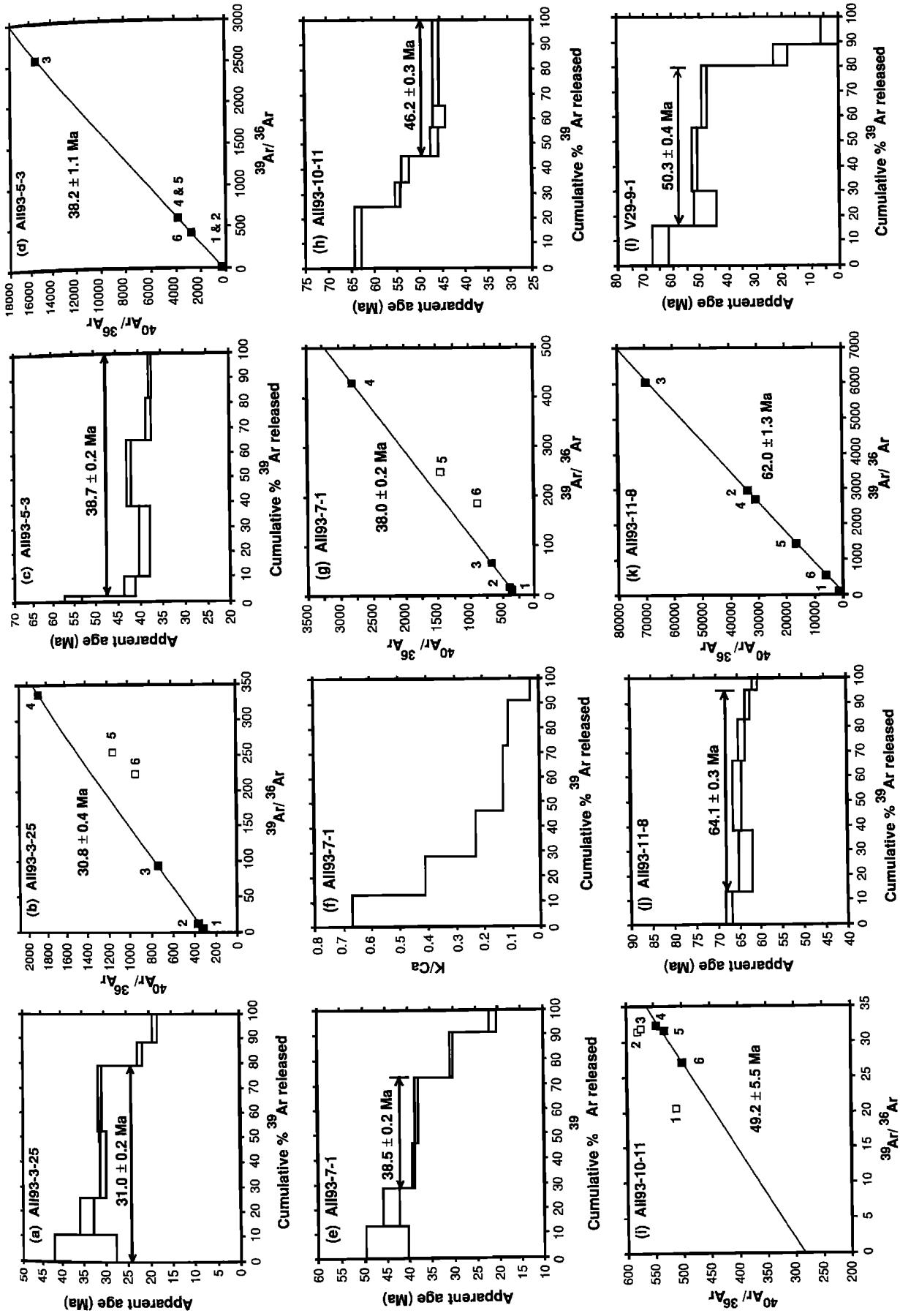

Fig. 3. Age-temperature spectra and $^{40}Ar/^{36}Ar$-$^{39}Ar/^{36}Ar$ correlation diagrams for basaltic samples from the Walvis Ridge. Age bands in spectra plots are the measured heating step ages ± 2σ. Errors on plateau ages are ± 1σ. The numbered points on the correlation diagrams correspond to the individual heating steps. Solid boxes in correlation diagrams indicate heating steps used in isochron calculations. A single representative K/Ca release spectrum diagram is also shown.

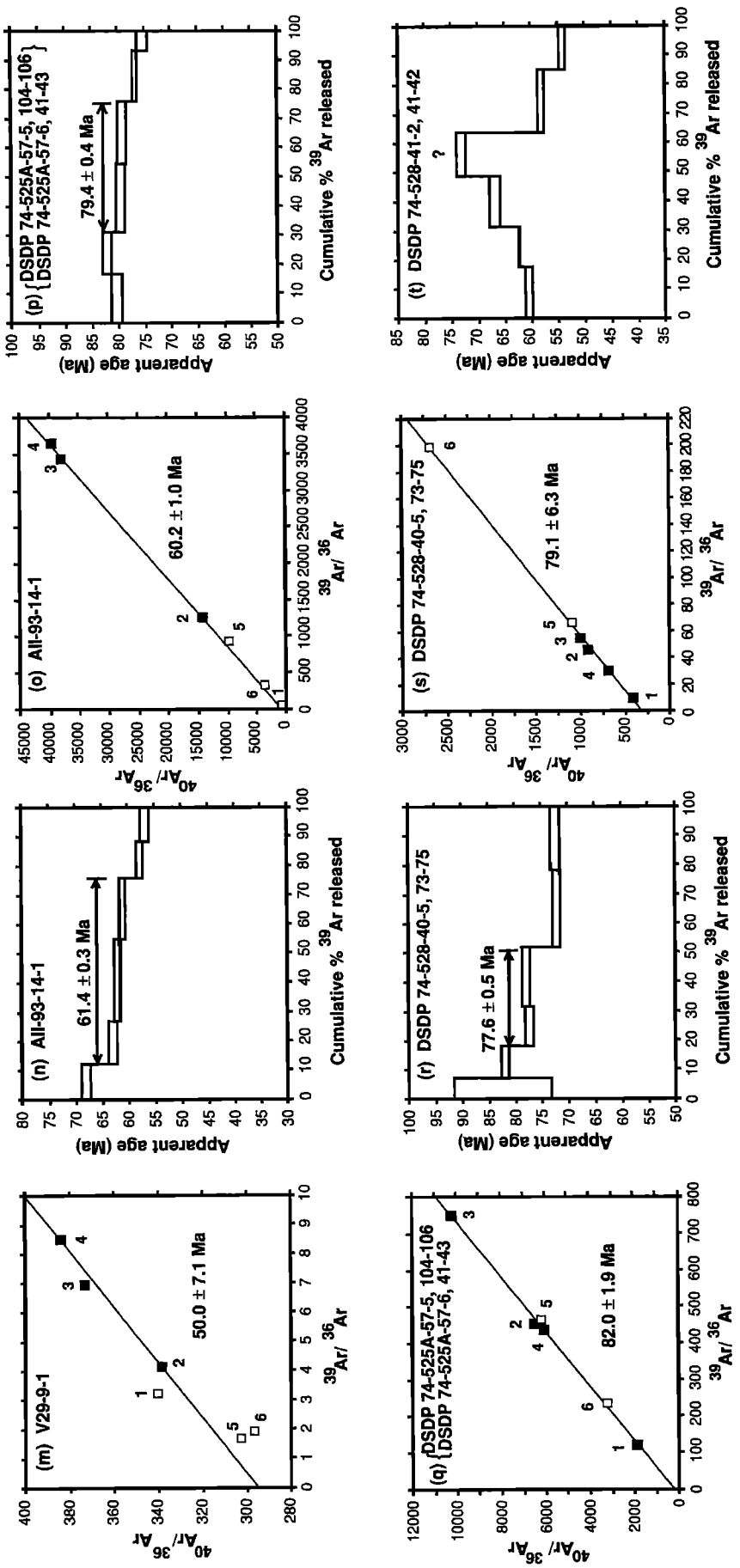

Fig. 3. (continued)

recovered from sites 525A and 528 are broadly constrained by magneto-biostratigraphic information from the overlying sediments [*Manivit*, 1984; *Chave*, 1984]. These data provide minimum estimates on the formation ages of the underlying basement and so act as an independent control on ^{40}Ar-^{39}Ar incremental heating age determinations.

Rock chips from core intervals DSDP 74-525A-57-5, 104-106 and DSDP 74-525A-57-6, 41-43 were combined, yielding a convincing middle temperature plateau age of 79.4 ± 0.4 Ma (62.3% of the total ^{39}Ar released) (Figure 3*p*), an isochron age of 82.0 ± 1.9 Ma (intercept of 288 ± 128) (Figure 3*q*), and a recalculated total fusion age of 79.1 ± 0.4 Ma. The apparent age of DSDP 525A basement is 79 Ma. This ^{40}Ar-^{39}Ar incremental heating age is compatible with the biostratigraphically constrained early Maestrichtian to late Campanian (between ~73 and 78 Ma) sediments which immediately overlie site 525A basement [*Manivit*, 1984]. Magnetostratigraphic correlation indicates that 525A basement formed within magnetic C32 (~ 72 to 74 Ma) [*Chave*, 1984].

Sample DSDP 74-528-40-5, 73-75 (located to the northwest of DSDP site 525A) produced an indistinct age-temperature plateau of 77.6 ± 0.5 Ma (33.6% of the total ^{39}Ar released) (Figure 3*r*), an isochron age of 79.1 ± 6.3 Ma (intercept of 297 ± 45) (Figure 3*s*), and a recalculated total fusion age of 75.9 ± 0.5 Ma. A best estimate of the apparent crystallization age at this site is between 78 and 79 Ma. This radiometric age range is somewhat older than the age of overlying sediments, which have been biostratigraphically constrained at middle Maestrichtian age (between ~72 and 69 Ma) [*Manivit*, 1984], with a corresponding magnetostratigraphic assignment of C31 to C32 times (~ 69 to 74 Ma) [*Chave*, 1984].

The age-temperature release spectrum of sample DSDP 528-41-2, 40-42 contrasts with the generally plateaulike or inverse staircase release spectra which are characteristic of the samples examined in this study. Heating step ages increase to a maximum for a middle temperature step (73.2 ± 0.4 Ma) and then decrease again to approximately the age of the first heating step, so forming an arched release pattern (Figure 3*t*). This age-release spectrum may reflect significant loss of $^{40}Ar^*$ from this sample. The recalculated total fusion age is 62.5 ± 0.3 Ma, which is substantially lower than the radiometric age of the overlying sample (DSDP 528-40-5). It was therefore concluded that the apparent total fusion age of DSDP 528-41-2 is erroneously young; this result clearly demonstrates the pitfalls of conducting single step total fusion rather than incremental heating ^{40}Ar-^{39}Ar experiments on seawater altered whole rock basalts. Such an arched release spectrum (Figure 3*t*) may prove to be characteristic of such erroneously young total fusion ages.

Sample AII-93-21-1, recovered from the most northeasterly of the sample sites investigated in this study, produced an extreme example of an inverse staircase age-temperature spectrum, and did not produce a recognizable age plateau. The percentage of radiogenic ^{40}Ar released during incremental heating was low, 60% being the maximum value attained. The recalculated total fusion age of 69.8 ± 0.8 Ma is the best age estimate for this sample site; this apparent age probably represents a minimum estimate, rather than the true sample age.

The oldest age determined for the Walvis Ridge is provided by DSDP 363, where drilling encountered lower Aptian (about 113 to 119 Ma) sediments, a short distance above the inferred basaltic basement [*Bolli et al.*, 1978]. To a first approximation the age of Walvis Ridge basement increases linearly with increasing distance from Tristan da Cunha (Figure 4), thus linking recent hot spot volcanism on Tristan da Cunha, via the Walvis Ridge, to its 120-130 Ma expression on the Namibian coast, the Etendeka continental flood basalt field.

Rio Grande Rise

Samples DSDP 516F-128-1, 22-24 and DSDP 516F-128-1, 104-107 both failed to produce conclusive plateau ages. The first

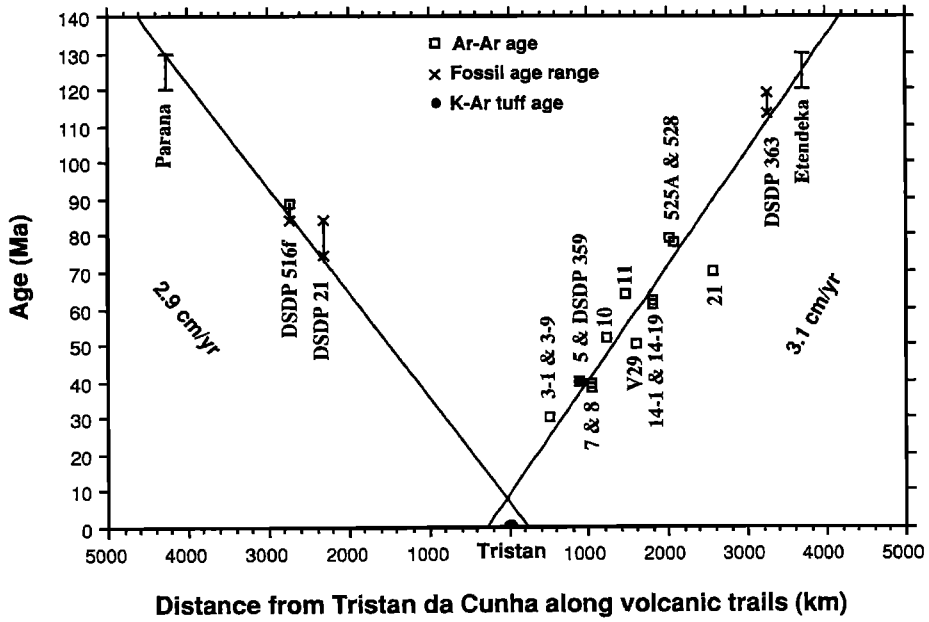

Fig. 4. All available basement age constraints for the Walvis Ridge and Rio Grande Rise are plotted against their respective distances along volcanic trail, from Tristan da Cunha. A straight line has been fitted to these data, with an age of 0 Ma assigned to Tristan da Cunha. Migration rates for the African and South American plates over the Tristan plume have been estimated at 3.1 and 2.9 cm/yr, respectively.

yielded a recalculated total fusion age of 88.7 ± 0.5 Ma and an isochron age of 87.2 ± 8.9 Ma (intercept of 293 ± 42). The second produced an even more extreme example of an inverse staircase release pattern, with a recalculated total fusion age of 95.5 ± 0.5 Ma. An apparent age of 88 Ma was chosen as the best available constraint on the time of crystallization of this site. DSDP 516F basalts were sampled beneath poorly lithified and recrystallized sediments which have been biostratigraphically dated at between Coniacian to Santonian age (84 Ma to 88.5 Ma) [*Weiss*, 1983]. Since this time was within the long Cretaceous normal magnetization period, magnetic stratigraphy is not informative. *Musset and Barker* [1983] also investigated DSDP 516F basalts using the ^{40}Ar-^{39}Ar incremental heating method and concluded that 86.0 ± 4.0 Ma was the best estimate of the age of crystallization.

DSDP site 21, located on the northeastern shoulder of the Rio Grande Rise (Figure 6), provides a minimum biostratigraphic age of Campanian time (74.5 to 84 Ma) for the underlying basement. This drill hole did not actually reach basement but terminated in shallow water sediments consisting mainly of megafossil fragments; the actual thickness of this rock layer is unknown [*Bukry and Bramlette*, 1970; *Gartner*, 1970; *Blow*, 1970]. The distribution of available Rio Grande Rise basement and fossil ages, in conjunction with present estimates of the narrow age-range of the Parana flood basalts, is compatible with age-progressive volcanism linking the northeastern shoulder of the Rio Grande Rise (~75 to 84 Ma) to 120-130 Ma continental flood basalt volcanism (Figure 4).

However, volcanism may not have migrated along the Rio Grande Rise in a simple, linear age-progressive fashion. Portions of the Rio Grande Rise–Walvis Ridge system appear to have developed in a manner similar to that of present day Iceland [*Vogt and Johnson*, 1975; *Saemundsson*, 1979; *Helgason*, 1985] and Figure 9*b*. *Barker* [1984] has observed that a sequence of planar dipping reflectors exists beneath the reflector associated with the basalt at the base of DSDP 516F, located on the Rio Grande Rise plateau. When Icelandic plateau basalts eventually become submerged, they will show similar characteristics. Such a dipping reflector sequence is similar to those found along many continental margins and is usually considered to represent a subaerial seafloor spreading facies, composed of sheet lava flows and shallow marine or alluvial sediments. The central plateau of the Rio Grande Rise may therefore have formed along a spreading-axis, which in turn was astride, or in close proximity, to a hot spot, as is the case for Iceland today. Numerous eastward spreading-axis jumps were, in all probability, associated with the formation of the central plateau of the Rise. The eastern, N-S ridge of the Rio Grande Rise has previously been attributed to the eruption of hot material along a segment of the South Atlantic spreading-axis [e.g., *Vogt and Johnson*, 1975]. The history of interaction between the spreading-axis and the Tristan hot spot is reconstructed in a later section.

An additional complication to understanding the evolution of the Rio Grande Rise arises from an undefined volume of Eocene volcanism identified by *Bryan and Duncan* [1983], who have dated volcanoclastic, turbiditic horizons at 46 Ma, using the K-Ar dating technique. This enigmatic second phase of volcanism has presently no satisfactory explanation within the context of the hot spot model proposed for the formation of the Walvis Ridge–Rio Grande Rise.

Eruption rates through time of Walvis Ridge–Rio Grande Rise volcanism have yet to be quantitatively estimated. However, significantly more material was emplaced when the spreading-axis was in close proximity to the hot spot (Figure 9*b*): the contribution from renewed volcanism on the Rio Grande Rise plateau during the Eocene should be kept in mind when making such an assumption. An obvious explanation is that the Tristan plume decreased in strength through time. Changing eruption rates may also reflect the changing tectonic character of the overriding plate, into which the Tristan magmas were emplaced (i.e., from rifting continental crust, to spreading-axis, to finally, an intraplate environment). Changes in plate thickness and/or velocity may have controlled, in part, the volumes of Tristan magma which erupted. Variations in the dynamics of the plume, and the surrounding mantle, could also have played a contributory role.

Absolute Motion Modeling (Fixed Hot Spot Reference Frame)

Rotation Parameters for African Plate Motion Over Hot Spots

Previously estimated sets of reconstruction parameters for African plate motion over fixed hot spots (i.e., absolute motion) [*Morgan*, 1981, 1983; *Duncan*, 1981] have been adjusted such that the predicted trail of the African plate over the Tristan hot spot would reconstruct the distribution of Walvis Ridge basement ages (Figures 5 and 6). The geographical coordinates of the adjusted rotation poles were located geometrically by requiring that small circles, when fitted about each pole, should simultaneously fit the geometry of three African plate hot spot lineaments: the Walvis Ridge and the volcanic trails of the Reunion and Marion hot spots. This is illustrated by the fact that the geometry of the predicted tracks for the Tristan, Reunion and Marion hot spots, coincides with that of their postulated volcanic trails (Figure 7). The Africa/hot spots reconstruction parameters given in Table 3 differ from those of earlier versions, primarily in that the rates of plate motion are now constrained to match the distribution of new basement ages along the Walvis Ridge. The geometry of the predicted trails of the St. Helena and Comores hot spots is also in broad agreement with that of their postulated volcanic trails (Figure 7).

The principal assumptions made in this particular model are: (1) the Walvis Ridge basement ages and geometry perfectly record the motion of the African plate over hot spots, (2) the ocean island of Tristan da Cunha represents the center of a discrete, small diameter, vertically rising plume, as do the islands of Reunion, and Marion, (3) the geometry of the Reunion, Marion/Prince Edward hot spot trails is accurately known, and (4) there has been no significant wander of these three hot spots with respect to one another.

The Predicted Trail of the Tristan Plume Compared to Walvis Ridge Bathymetry and Age Data

Figure 5 illustrates the relationship between the modeled trail of the African plate over the Tristan plume and the bathymetry and distribution of all available Walvis Ridge basement ages. A 30 Ma seamount cluster, located due east of Tristan da Cunha, tightly constrains the rotation angle about the 30 Ma finite reconstruction pole. As no volcanic trail is evident between this 30 Ma site and the island of Tristan da Cunha, the 10 and 20 Ma reconstruction poles were calculated by interpolation. The rotation angle about the 40 Ma is very well constrained by age data from three sample sites, and a supporting K-Ar age.

The 50 to 70 Ma portion of the Walvis Ridge consists of a complex series of subparallel volcanic lineaments (Figure 5). It is

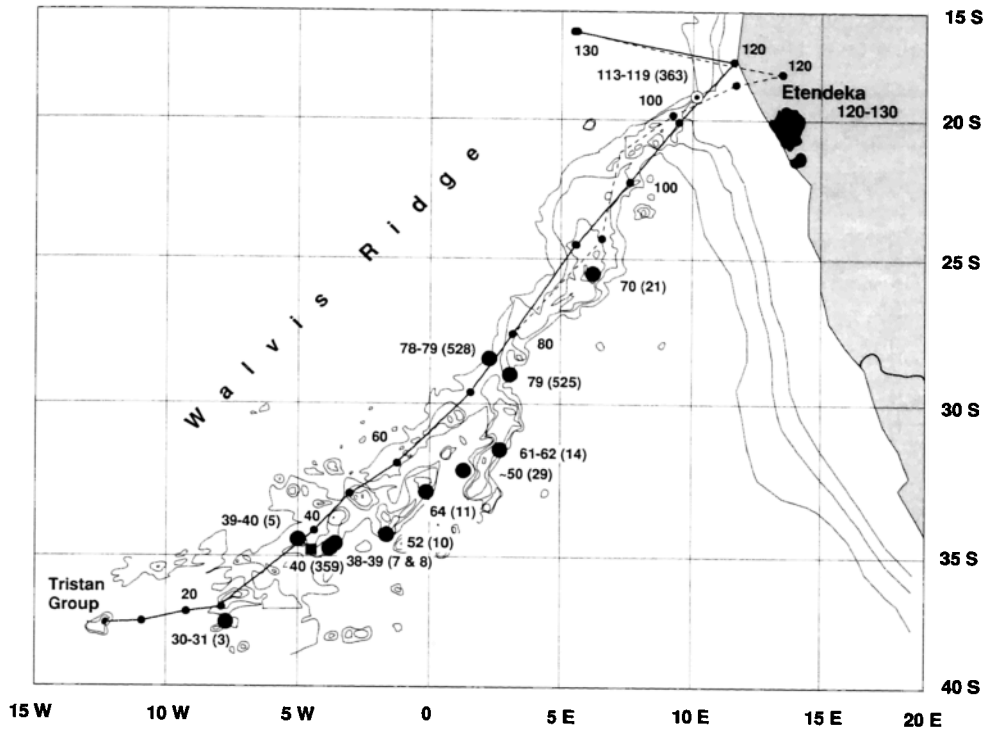

Fig. 5. The direction of modeled African/hot spots motion is shown by the heavy line connecting Tristan da Cunha (0 Ma volcanism) to the 120 to 130 Ma Etendeka continental flood basalts. The small solid circles distributed along this line represent the modeled progress of the African plate over the Tristan hot spot at intervals of 10 Ma. Sample sites are shown as large solid circles, along with ages, and site labels in parentheses. Two reconstructions from the period 80 Ma to 120 Ma are presented; the dashed hot spot track follows the geometry of the Walvis Ridge (model B), whereas the solid track (model A) is a linear, best fit to the bathymetry of the northern portion of the Walvis Ridge. The 130 Ma interval point on the hot spot tracks reconstructs the Etendeka basalts to the southeastern edge of a hypothetically large diameter plume, which may have existed at the time of continental rifting. Mercator projection.

somewhat of a quandary as to which of these minor ridges best records the motion of the African plate over the Tristan hot spot. The northern lineament formed along a spreading-axis, in contrast to the two southern lineaments, which formed in an intraplate situation, as will be shown in a later section. While these southern lineaments may in fact accurately record the motion of the African plate over the Tristan plume, the rotation parameters given in Table 3 have been constrained so as to predict a hot spot trail which follows the northern limb. These rotation parameters predict smooth, linear hot spot trails for other African hot spots which are compatible with the geometry of their postulated volcanic traces. As no basement ages were available for the northern limb, reasonable estimates were made on the basis of the age data available for the southern two limbs, in order to constrain the angles of rotation about the 50, 60, and 70 Ma reconstruction poles. However, significantly more basement sampling is obviously essential in order to better define the tectonic and geochemical evolution of this, and other such complex tectonic regions of the Walvis Ridge–Rio Grande Rise system; increased sampling will reveal which specific portions of the volcanic trails best record the motion of the African plate over the hot spot. The rotation angle about the 80 Ma finite reconstruction pole is well constrained by the 78-79 Ma DSDP transect of the Walvis Ridge.

Between 80 and 120 Ma little reliable age data are available; the enigmatic 70 Ma age for sample AII-93-21 was interpreted as a minimum age and therefore was not used in the estimation of rotation parameters. However, future studies may confirm that reactivation of the volcanic lineament may actually have occurred in this region of the Walvis Ridge. Two sets of rotation parameters have been estimated for Africa/hot spot motion for the period 80 to 120 Ma (Figure 5). Model A predicts a track which follows the bathymetry for this portion of the Walvis Ridge in basically a linear fashion. In contrast, the track predicted by model B closely follows the curvature of the Walvis Ridge. If, indeed, this section of the Walvis Ridge–Rio Grande Rise system represents a twin of present day Iceland (to be discussed in the following section), the changing curvature of the Walvis Ridge does not, in all probability, record changes in the direction of African plate motion over hot spots. Following this reasoning, model A is a preferable model and so will be used in following discussions.

At ~130 Ma the initial expression of the Tristan plume on the surface of the rifting African and South American plates was in the form of the Parana–Etendeka continental flood basalt (Figure 9*a*). These lavas may have erupted in response to the rapid partial melting of the large diapiric head of the Tristan plume [*Richards et al.*, 1989]. Subsequent volcanism linked to the Tristan plume, i.e., the Walvis Ridge–Rio Grande Rise, are possibly related to smaller volumes of plume material rising through the conduit or "tail", formed by the diapir. Alternatively, the Parana-Etendeka basalts may have been formed by the pressure-release melting of the upper mantle, which would have occurred if continental rifting commenced in a region warmed by a hot spot, previously unable to penetrate the lithosphere [*White and McKenzie*, 1989; *Cox*, 1989]. A 130 Ma Africa/hot spots

TABLE 3. Finite Reconstruction Poles for African Plate Motion Over Hot Spots

Age, Ma	Latitude, °N	Longitude, °E	Angle*
Model A (Linear Fit Through NE Walvis Ridge)			
10	52.0	-16.3	-1.0
20	51.4	-24.3	-2.4
30	51.5	-23.3	-3.5
40	47.3	-45.9	-7.1
50	45.7	-50.9	-8.7
60	44.9	-50.7	-10.6
70	43.6	-54.2	-14.0
80	42.4	-57.5	-16.4
90	40.0	-59.6	-20.2
100	39.7	-60.6	-23.2
110	39.4	-61.3	-26.0
120	41.5	-64.9	-29.2
130	32.8	-73.3	-26.4
Model B (Following the Curvature of NE Walvis Ridge Bathymetry)			
90	41.2	-58.7	-21.0
95	38.6	-64.2	-23.8
100	40.2	-64.5	-26.1
110	40.9	-61.6	-28.5
120	41.1	-58.0	-30.0

*Negative angles indicate counterclockwise rotation.

reconstruction pole was estimated such that the Etendeka basalt field would straddle, on reconstruction, the eastern edge of such a large hot spot (Figure 9*a*).

An additional constraint on the reliability of the adjusted rotation parameters is that the predicted trail of the South American plate over the Tristan plume should be in reasonable agreement with the evolutionary history of the Rio Grande Rise, as it is presently understood. South American plate motion over hot spots has been reconstructed by the addition of South America/Africa finite reconstruction poles [*Cande et al.*, 1988] to African motion over hot spots. Figure 6 shows that the hot spot track predicted by model A trends in a linear, NW-SE direction through the Rio Grande Rise. Model B, which more closely follows the bathymetry of the Walvis Ridge, predicts a more northerly trending track until 100 Ma when it changes direction to the west. Africa/hot spots rotation parameters do not predict a trail for the South American plate over the Tristan plume, which follows the N-S ridge of the eastern Rio Grande Rise (Figure 6). However, as will be shown in a later section, this portion of the rise probably formed along a southwardly propagating spreading-axis (Figure 9*b*), and so did not record the true direction of South American plate motion over the Tristan hot spot. This point illustrates the critical importance of accurately understanding the evolutionary history of individual hot spot-related volcanic trails, in the estimation of valid absolute motion reconstruction parameters.

Support for a NW-SE trending hot spot track through the Rio Grande Rise is provided by recent studies of the South Atlantic geoid. At short wavelengths, seafloor topography and variations in the geoid are strongly correlated and so provide a better constraint on seafloor topography in poorly surveyed areas, such as the South Atlantic. A map of short-wavelength regional undulations in the amplitude of the geoid shows a good

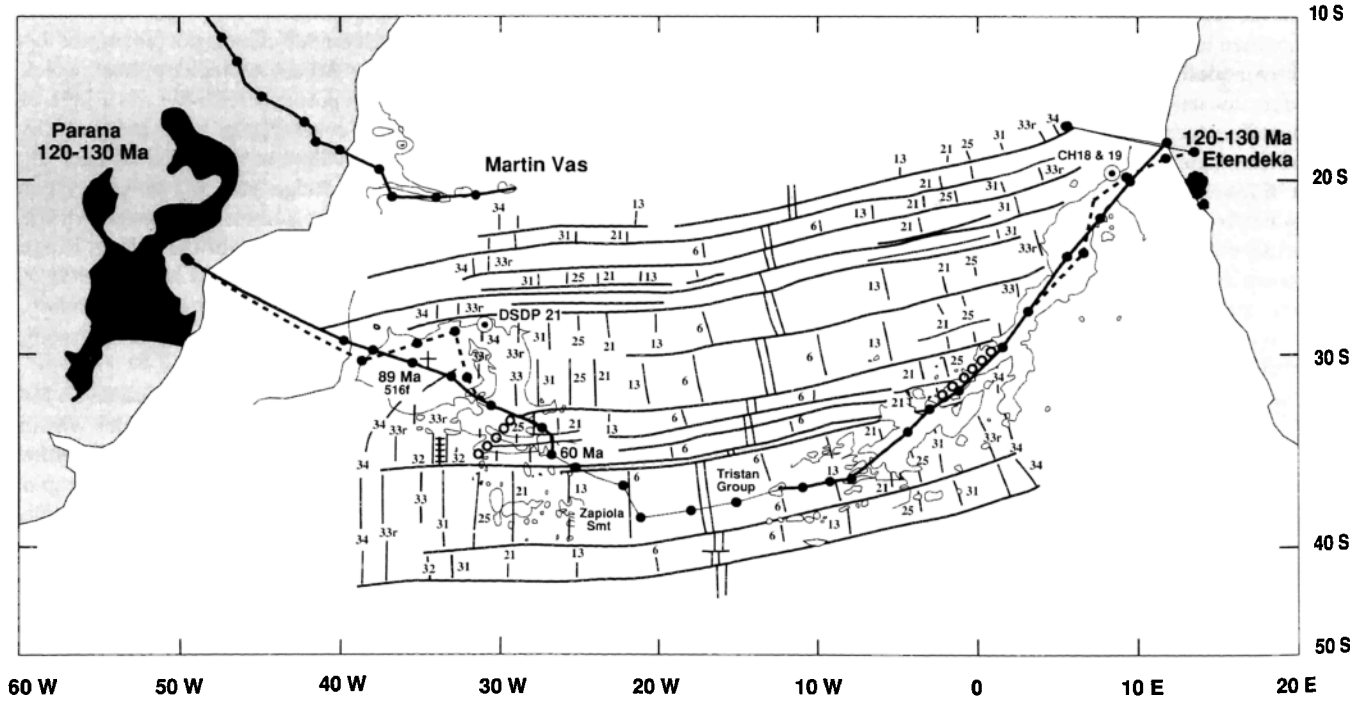

Fig. 6. Predicted trail of the African and South American plates over the Tristan hot spot. South American/African relative motion [*Cande et al.*, 1988] was added to Africa/hot spots motion given in Table 3. The modeled trail of the Martin Vas plume is also shown. Mercator projection.

correlation between the bathymetry of the Walvis Ridge and its topography determined from the geoid [*Gibert et al.*, 1989; Plate 1]. The geoid-inferred topography of the Rio Grande Rise, however, forms an elongated NW-SE trending lineament, as predicted by the hot spot track, which does not correlate well with available bathymetry (Figure 1*b*). A NW-SE trending volcanic trail is more symmetrical with respect to the Walvis Ridge than is the bathymetry of the Rio Grande Rise. *Fleitout et al.* [1989] have detected numerous small-wavelength elongated features on filtered geoid and topography maps of the South Atlantic. A number of these features are orientated at N50°E for the African plate, and N65°W for the South American plate: this agrees with the geometries of the predicted hot spot trails shown in Figure 6. The authors attribute these elongated features to magmatic traces left over a large number of convecting plumes, which record the directions of African and South American absolute plate motions.

African and South American Plate Motions Over South Atlantic and Indian Ocean Hot Spots

The island of Reunion is composed of two volcanoes, the dormant Piton des Neiges (>2 to 0.02 Ma [*McDougall*, 1971; *Chevallier and Vatin-Perignon*, 1982; *Gillot and Nativel*, 1984]) and Piton de la Fournaise, which began to erupt earlier than 0.5 Ma and is presently one of the most active volcanoes in the world [*McDougall*, 1971; *Gillot and Nativel*, 1989]. *Morgan* [1981] proposed that Reunion locates a hot spot, which formed the island of Mauritius (7-8 Ma [*McDougall*, 1971]) and the volcanic ridge extending northward beneath the Mascarene Plateau. On the Indian plate, the trail of the Reunion hot spot consists of the Chagos Bank, the Maldive and Laccadive islands, and the Deccan continental flood basalts. Thus, the track of the Reunion hot spot stretches for ~5,000 km from Reunion to the flood basalts of western India. The age progressive character of this hot spot lineament has been confirmed by recent biostratigraphic and magnetostratigraphic data [*Backman et al.*, 1988], radiometric dating [*Duncan and Hargraves*, 1990], and isotopic studies [*White et al.*, 1990]. Biostratigraphic and magnetostratigraphic information provides an age estimate of between chrons C13N-1 and C13N-2 time (~36 Ma) for Ocean Drilling Program (ODP) site 706 basalts, located at the northeastern margin of the Nazareth Bank (Figure 7). Extending northward from this plateau is the Saya de Malha Bank, dated at 47 Ma by ^{40}Ar-^{39}Ar radiometric age determination of basalt recovered from industrial drill site SM-1 (located between ODP sites 706 and 707, Figure 7). *Duncan and Hargraves* [1990] have shown that this bank

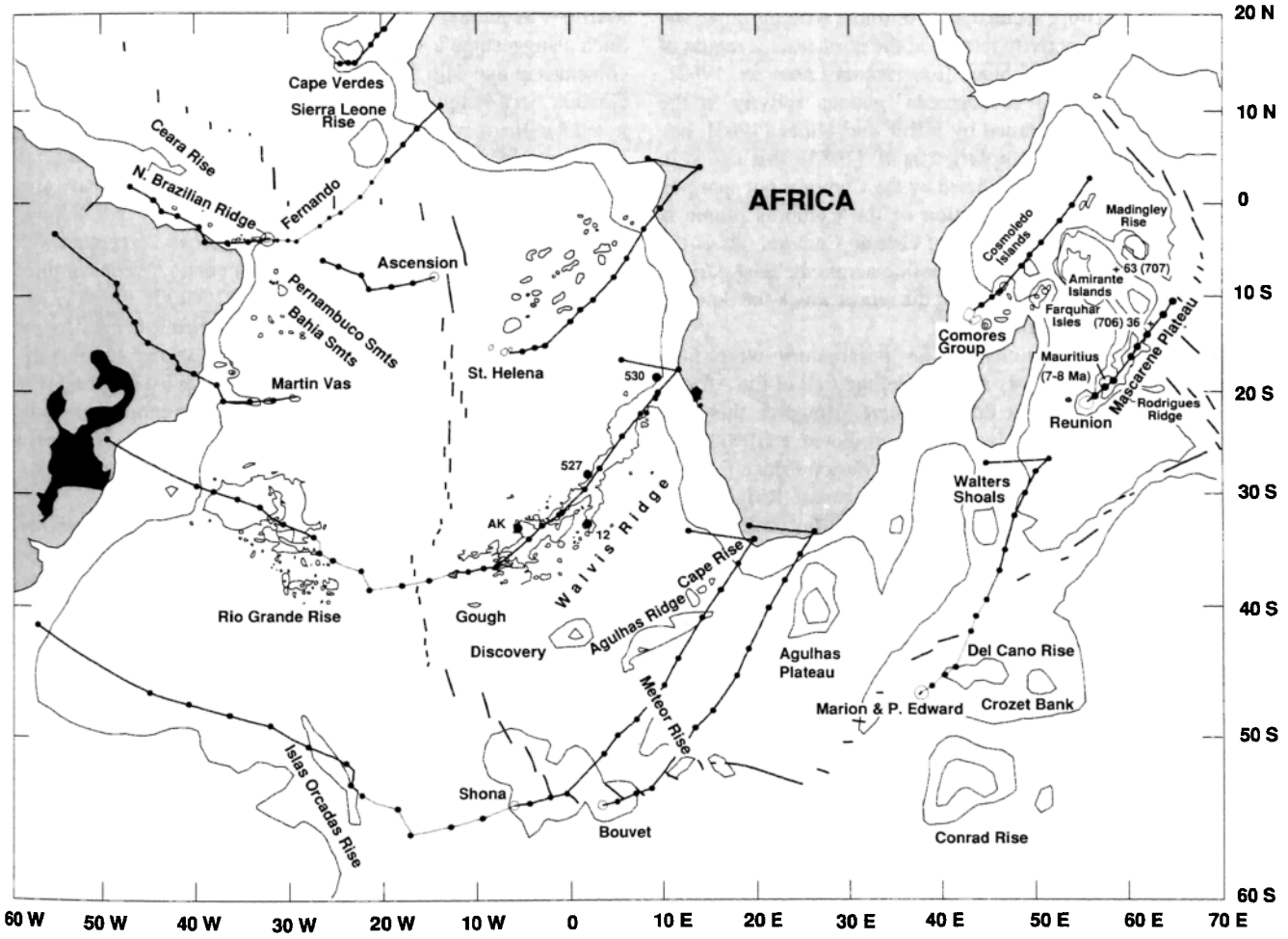

Fig. 7. The trails of all South Atlantic and Indian Ocean hot spots located on the African and South American plates are shown. Thin portions of modeled hot spot tracks illustrate the connection between volcanic trails which are linked to a common hot spot, and do not correspond to actual volcanic trails. Biostratigraphic and magnetostratigraphic ages shown for the Mascarene Plateau are from *Backman et al.* [1988]; drill site numbers are shown in parentheses. K-Ar age range for Mauritius is from *McDougall* [1971]. Mercator projection.

formed simultaneously with the Chagos Bank (48 Ma) on the Indian plate, and that these features were separated by the initiation of seafloor spreading at about 36 Ma along the Central Indian Ridge. The volcanic ridge connecting the Saya de Malha Bank with the Seychelles Bank has been biostratigraphically and magnetostratigraphically dated at ODP site 707 as C26R, between 62 and 63 Ma, and at ~64 Ma by radiometric dating. This ridge is considered to have formed along the southwestern edge of the Deccan Traps, and to have been rifted away from India as the Arabian Sea began to open (*Duncan and Hargraves*, 1990].

The Africa/hot spots reconstruction parameters given in Table 3 have been estimated in such a manner as to predict a trail for the Reunion plume that would follow the geometry of the Mascarene Plateau (for the period between 0 and about 36 Ma). However, the predicted rate of migration of the African plate over the Reunion plume (Figure 7) is somewhat slower than that indicated by available basement age data for its volcanic trail (Figure 7). Relative motion between the Reunion and Tristan hot spot could explain this misfit. An alternative explanation might involve relative motion across the east African rift zone, i.e., the western boundary of the Somalia plate, which could have added an easterly component of motion to Somalia plate migration over the Reunion plume [*Emerick and Duncan*, 1982].

The geometry of the predicted trail of the Comores hot spot is in general agreement with that of its postulated volcanic trail, the Comores, Cosmoledo, Farquhar and Amirante island groups, and the Tertiary igneous activity located at the northeastern region of the Seychelles continental block [*Emerick and Duncan*, 1982]. This intense episode of widespread igneous activity in the Seychelles Islands, first noted by *Baker and Miller* [1963], has been dated at 63 Ma by *MacIntyre et al.* [1985]; this age is in good agreement with that predicted by the Comores hot spot trail (Figure 7). The zero age location of the Comores plume is assumed to be beneath the island of Grande Comore. As is the case with the Reunion hot spot, extension across the East African rift zone could also have augmented the rate at which the Somalia plate migrated over this hot spot.

Africa/hot spots reconstruction parameters were also constrained to follow closely as possible, the trail of the African plate over the Marion/Prince Edward plume. However, there is a small degree of misfit between the predicted trail and the somewhat indistinct volcanic trail of the Marion/Prince Edward plume, the Walters Shoals and the Madagascar Ridge. The postulated zero age location of this hot spot trail is the volcanically active Marion Island, located on the Antarctica plate (Figure 7).

Hartnady and le Roex [1985] have proposed the existence of a hot spot, known as Shona, located near the southernmost tip of the South Atlantic spreading-axis, in close proximity to the Bouvet hot spot (Figure 7). The authors support the existence of such a hot spot with geochemical data, which distinguish between the composition of Bouvet and Shona magmas. The zigzag shape of the Cape Rise–Meteor Rise lineament has been attributed to the crossing of the Shona hot spot by the active transform segment of the Falkland-Agulhas Fracture Zone in Late Mesozoic times [*Hartnady and le Roex*, 1985]. The relationships between the predicted trail of the Shona hot spot, on the African and South American plates, and the geometries of the Meteor and Islas Orcadas Rises, respectively, suggest that both of these features were formed simultaneously, at about 60 Ma (as suggested by *LaBrecque* [1986]) by the Shona hot spot (Figure 7). Basal sediments on the Islas Orcadas Rise (ODP site 702) show that this feature is >61 Ma and so is possibly Late Cretaceous [*Ciesielski et al.*, 1988]. The oldest in-situ or reworked microfossils at ODP site 703, located on the Meteor Rise are Eocene, in contrast to the Late Cretaceous microfossils found on the Islas Orcadas Rise [*Ciesielski et al.*, 1988]. This age difference has been attributed to the Meteor Rise having experienced more recent volcanism, which would account for its shallower basement and more rugged relief. An additional constraint on the age of these features is given by the fact that the oldest anomaly bounding the east side of the Islas Orcadas Rise, and the corresponding west side of the Meteor Rise, is anomaly 24 (55 Ma) [*Cande et al.*, 1989].

The Trinadade–Columbia seamount chain represents the trail of the South American plate over the Martin Vas hot spot [*Herz*, 1977] (Figure 6). Ages of 0.7 Ma and 0.2 to 3 Ma have been determined for Martin Vas and its adjoining island to the west, Trinadade, respectively [*Herz*, 1977]. The predicted trail of this hot spot follows the Trinadade–Columbia seamount chain and broadly agrees with the 42-52 K-Ar age range determined for the Abrolhos archipelago, located somewhat to the north of the Trinadade–Columbia lineament [*Herz*, 1977, Figure 1]. In addition to the Abrolhos archipelago, the Hotspur, Rodgers, and Minerve Seamounts are located along the northern fringe of the Trinadade–Columbia seamount chain, while to the south, is located the Almirante Saldanha seamount [*Cherkis et al.*, 1989]. This broad zone of seamounts may indicate that, as the continental margin of the South American plate migrated over the Martin Vas plume, a wide diameter hot spot was in existence. Such a suggestion is supported by the fact that this hot spot track coincides in age with a group of alkalic igneous intrusions on the Goiania Arch ranging in age from 70 to 95 Ma [*Neill*, 1973], as noted by *Hartnady and le Roex* [1985]. About 200-300 km southeastward, a series of alkalic intrusions between Pocos de Caldas (63-80 Ma) and Cabo Frio (51 Ma) [*Neill*, 1973] have also been attributed to the Martin Vas plume [*Hartnady and le Roex*, 1985]; these continental intrusives are in broad agreement with the ages predicted for the Martin Vas hot spot. A series of three dated kimberlite deposits (80, 86 and 122 Ma) [*Crough et al.*, 1980, Figure 6] also coincide with the predicted trail ages for the hot spot. In addition, *Crough et al.* [1980] pointed out that the trail of the Martin Vas hot spot coincides with most of the alluvial diamond deposits in Brazil. The ages of these alluvial deposits are still uncertain, however, some geological evidence suggests a Cretaceous age [*Svisero et al.*, 1979], but other deposits are considered to be Precambrian.

The modeled trail of the St. Helena hot spot follows the southern boundary of its postulated volcanic trail, a broad NE-SW swath of seamounts and ridges. K-Ar ages of between 14 and 8 Ma have been determined for St. Helena [*Baker et al.*, 1967], although new data indicate an age range of between 9-7 Ma [*Chaffey et al.*, 1989]. The misfit between the predicted trail of the St. Helena plume and its volcanic trail may be explained by uncertainty in accurately locating the zero age center of the upwelling plume. An alternative explanation could be that Helena and Tristan hot spots are of significantly wider diameters (~500 km) than has been assumed for the purposes of this discussion [*O'Connor*, 1989].

An age range of 1.81 to 12.3 Ma has been determined for the island of Fernando de Noronha [*Cordani*, 1970]. The modeled trail of the Fernando de Noronha hot spot on the African plate coincides with the Sierra Leone Rise, although the predicted trail passes somewhat to the south of this feature (Figure 7). On the basis of both ocean drilling, and its distance from the spreading-axis, *Kumar and Embley* [1977] suggested that the Ceara Rise originated in conjunction with the Sierra Leone Rise,

at approximately 80 Ma, as shown by *Sibuet and Mascle* [1978]. The predicted trail of the African plate over the Fernando plume supports the suggestion that the Ceara and the Sierra Leone rises were formed simultaneously by the Fernando hot spot, at about 80 Ma (Figure 8); the North Brazilian Ridge may also have been formed by this particular plume. At the intersection of the Fernando de Norhona lineament and the South American continent near Fortaleza, Tertiary volcanic centers have been identified and attributed to the Fernando hot spot [*Almeida*, 1958; *Vandoros and Oliveira*, 1968]. Rb/Sr ages yielded an age of 34 ± 2 Ma [*Guimaraes et al.*, 1982], and five K-Ar analyses yielded an age of 28.7 ± 2.5 Ma. [*Vandoros and Oliveira*, 1968]. Recent K-Ar dating of these volcanics indicates an age range of 26 to 36 Ma (unpublished data), in broad agreement with the age predicted by the trail of the Fernando hot spot (Figure 7).

Ascension Island is located on the South American plate, in close proximity to the mid-Atlantic spreading-axis (Figure 7). The presence of unweathered basalt flows suggests that there has been volcanic activity on this island within the past few hundred years. Nine K-Ar ages from widely distributed sample sites, range from ages too young to be accurately dated by the K-Ar technique, to a maximum of 1.9 Ma (unpublished data). Two undated seamounts located at 9° 04°S, 19° 40°W and 8°29°S, 17° 07.6°W, some 570 and 300 km west of Ascension, respectively [e.g., *Cherkis et al.*, 1989], are located along the predicted trail of the Ascension plume on the South American plate (Figure 7). The predicted ages of these two seamounts are ~20 and ~10 Ma, respectively.

North American Plate Motion Over Hot Spots

North American plate motion over hot spots has been reconstructed by the addition of North America/Africa finite reconstruction poles [Klitgord and Schouten, 1986] to Africa/hot spots motion (Table 3). A number of interesting observations can be made regarding various central Atlantic hot spot systems, on the basis of this adjusted absolute motion reconstruction (Figure 8).

The most prominent volcanic trail in the central Atlantic basin is the New England Seamount chain, which probably formed in association with the Muir and Corner seamount complexes (Figure 8). Radiometric ages for this seamount chain confirm

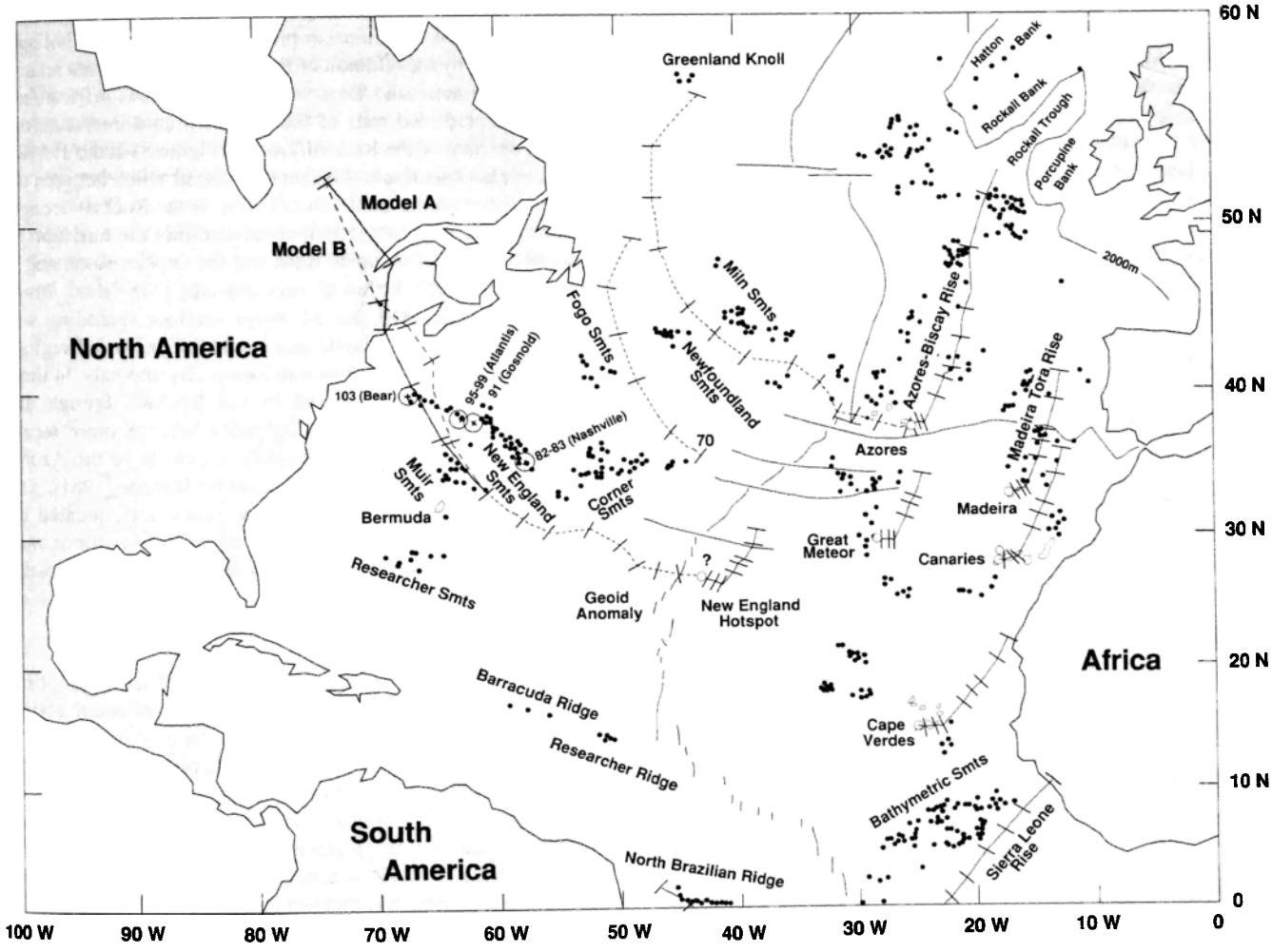

Fig. 8. The modeled trails of the African, North American and Eurasian plates over postulated hot spots. Tick marks along hot spot trails represent the progress of plates in 10 m.y. intervals. Relative motion parameters for North American/Africa motion [*Klitgord and Schouten*, 1986], and for Eurasia/North America [*Srivastava and Tapscott*, 1986] were added to African/hot spots motion (Table 3). The intermediate wavelength geoid anomaly shown is from *Vogt et al.* [1984]. Solid circles represent seamounts with a relief greater that 50 fathoms (300 feet) (91 m) [after *Epp and Smoot*, 1989]. Radiometric ages shown for the New England Seamounts are from *Duncan* [1984]. Mercator projection.

that it is age progressive [*Duncan*, 1984] (Figure 8). Previous authors have postulated that the zero age location of the New England hot spot is either the Great Meteor seamount, or a nearby location. However, this study indicates that a zero age position of the New England hot spot needs to be located at, or in the region of 27°N, 43.0°E, on the African plate, for the predicted trail of the North American plate over the New England hot spot to agree broadly with the geometry and distribution of radiometric ages along the New England Seamount lineament. The agreement between the geometries of the hot spot track and the volcanic lineament is nonetheless still poor. The Corner Seamounts formed when the spreading-axis was in close proximity to a hot spot between 80 Ma and 76 Ma [*Tucholke and Smoot*, 1990] and may also have been formed by the New England hot spot. Interestingly, this postulated location of the New England plume adjoins a large intermediate wavelength anomaly, which straddles the central Atlantic spreading-axis [*Vogt et al.*, 1984] (Figure 8). Such intermediate wavelength geoid anomalies generally coincide with major topographic structures such as subduction zones, mid-plate swells, and mid-oceanic ridges, and are considered to reflect sublithospheric processes. There is, however, no convincing evidence to support the existence of this plume from currently available studies of the isotopic and trace element composition of lavas erupting along this section of the mid-Atlantic spreading-axis [*Schilling*, 1986].

The Mesozoic plutonic complexes of northeastern North America, the White Mountain Intrusives of New England and the Monteregian Hills of Quebec, probably represent a continuation of the trail of the New England hot spot beneath the North American continent, as first proposed by *Morgan* [1972]. Regional uplift of southeastern Canada and New England in Cretaceous-early Tertiary time has been attributed to the passage of this region of the North American plate over a hot spot [*Crough*, 1981]. *Foland et al.* [1988] have reported that the Nd and Sr isotopic signatures of the parental magmas for the New England–Quebec continental plutons are similar to one another, regardless of whether the magma intruded Precambrian or Paleozoic crust, and also similar to those for the New England seamounts, described by *Taras and Hart* [1987]. *Foland and Faul* [1977] reported that K-Ar ages, supported by Rb-Sr and U-Pb data, indicate that the White Mountain Intrusives constitute distinct age groups of 230, 200-156, and 124-100 Ma. *Morgan* [1983] and *Crough* [1981] accounted for this grouping of ages by suggesting that a series of different hot spots have been active beneath the White Mountain region, with the most recent age period of volcanism associated with the New England hot spot. *Foland et al.* [1986] and *Gilbert and Foland* [1986] determined, on the basis of ^{40}Ar-^{39}Ar dating, that the Monteregian Hill centers formed within a short interval of time at 124 Ma. The age distribution along the New England–Quebec plutonic lineament is in very broad agreement with the hot spot track shown in Figure 8. However, it should be kept in mind that the 120 and 130 Ma rotation poles for Africa/hot spots, on which this reconstruction is based, are not well constrained.

The Great Meteor Seamount (30°N, 29°W) (Figure 8) may reflect the earlier location of a plume, now extinct, which formed the Newfoundland seamounts and/or Fogo Seamounts (Figure 8); both of these seamount complexes are located on Cretaceous Quiet Zone to older seafloor [e.g., *Klitgord and Schouten*, 1986]. The modeled track of this plume assumes a zero age for the Great Meteor Seamount; however, K-Ar ages of 11 Ma and 17 Ma have been determined [*Wendt et al.*, 1976]. An ^{40}Ar-^{39}Ar age of 97.7 ± 1.5 Ma has been determined for trachyte dredged from the Newfoundland seamount [*Sullivan and Keen*, 1977], compatible with the age predicted by the reconstruction of North American plate motion over a Great Meteor plume (Figure 8). Earlier activity caused by this hot spot may be marked by 115-145 alkaline intrusions along the coast of Newfoundland [*Clark*, 1977].

Using the empirical age-depth curve for the Atlantic Ocean crust, *Tucholke and Smoot* [1990] have shown that the Corner seamounts formed at about 80 Ma to 76 Ma, while on the African plate, the conjugate Cruiser plateau, formed at 76 Ma. Volcanism appears to have migrated northward from Great Meteor Seamount in early Cenozoic time, and then southward to Great Meteor Seamount in the late Cenozoic, with renewed volcanism occurring on some of these seamounts 20 to 30 Ma after their initial formation over a hot spot. The existence of "intralithospheric conduits" of several hundred kilometers in length may have maintained a link between these seamounts and the hot spot [*Tucholke and Smoot*, 1990]. If plume material from the Great Meteor and New England plumes were supplied simultaneously to the spreading-axis between 80 Ma and 76 Ma, the combined flow of magma from these two hot spots might account for the construction of the N-S elongated, Corner Seamounts–Cruiser Plateau (Figure 8).

The motion of the Eurasian plume over the Azores hot spot was calculated by the addition of Eurasian/North America relative motion [*Srivastava and Tapscott*, 1986] to that of African/hot spots. The predicted trail of the Azores plume intersects the southern opening of the Rockall Trough (Figure 8) at the 105 Ma location on hot spot track. This result suggests a link between the Azores plume and the initiation of rifting in the Rockall Trough. *Srivastava and Tapscott* [1986] concluded that the initiation of rifting between the Porcupine Bank and the Orphan Knoll and in the Rockall Trough began at anomaly M0 (118 Ma). From between anomalies M0 and 34 active seafloor spreading was initiated in the North Atlantic and Rockall Trough (all regions south of the Charlie Gibbs Fracture Zone). By anomaly 34 time, seafloor spreading had ceased in the Rockall Trough and commenced to the west in the Labrador Sea. A more recent expression of the Azores plume would appear to be the Azores Biscay Rise (Figure 8), as first suggested by *Morgan* [1981]. On the North American plate, the Milne seamounts, located on between approximately anomaly 32 to anomaly 34 seafloor, may record the trail of the Azores plume on the North American plate.

Hot Spot Fixity

The cornerstone of all hot spot or absolute motion reconstructions is the assumption that hot spots occur above plumes which rise from, as yet undefined, depth(s) in the mantle to the base of the lithosphere, and that such plumes remain fixed globally with respect to one another over geologically significant periods of time (e.g., 100 m.y.). However, a global extension of the finite reconstruction parameters presented here in order to further test this hypothesis, is beyond the scope of this paper. The research reported here has focused on estimating the most valid set of reconstruction parameters for African plate motion over hot spots, on the basis of presently available data for hot spot generated volcanic lineaments on the African plate. A better understanding of the history of interaction between the mid-Atlantic spreading-axis and the Tristan hot spot has contributed information as to how well particular portions of the Walvis

Ridge–Rio Grande Rise volcanic system actually record African and South American plate motions over the Tristan hot spot. Additional constraints on African plate motion over hot spots are, however, critical to further adjustments of African absolute motion. Ongoing radiometric and isotopic studies of basalts recovered from the St. Helena seamount lineament, the seamount chain extending eastward from Gough Island, and additional samples from the Walvis Ridge–Rio Grande Rise, should provide such additional constraints on African plate motion over hot spots [J. M. O'Connor et al., manuscripts in preparation]. Africa/hot spots reconstruction poles given in Table 3 (adjusted, if necessary, in the light of ongoing studies of South Atlantic volcanic trails) will be extended globally [J. M. O'Connor et al., manuscript in preparation]. Such a study will evaluate differing adjustments to Africa/hot spots reconstruction parameters and lead to a further test as to whether or not hot spots are fixed with respect to one another. While uncertainty ellipses, following the method of *Stock and Molnar* [1983], have not been calculated for the reconstructions discussed above, typical errors involved in extending African/hot spots motion globally through relative motion plate circuits are ± 100 km [*Molnar and Stock*, 1987].

Spatial Relationship Between the Spreading Axis and the Tristan Hot Spot

For the period of time when the Walvis Ridge–Rio Grande Rise system was forming in a synchronous, age-progressive manner (apart from possible Eocene reactivation), the mid-Atlantic spreading-axis must have been located astride, or in close proximity to the Tristan hot spot. Tristan da Cunha, which is situated on anomaly C6 (19 Ma) African plate seafloor, is located some 550 km east of the present day spreading-axis (Figure 2). This ~550 km separation between the spreading-axis and the hot spot points to a westward migration of the spreading-axis away from the plume. The absence of a volcanic trail linking the southeastern terminus of the Rio Grande Rise to Tristan da Cunha may best be explained in terms of such a westward migration of the spreading-axis, which eventually shut off the supply of hot material from the upwelling plume. The change in Walvis Ridge morphology from that of aseismic ridge to an indistinct line of discrete seamounts and guyots (Figure 1*a*) also reflects, no doubt, this transition from on-axis to intraplate volcanism.

In order to better illustrate the changing spatial relationship between the spreading-axis, the hot spot, and the evolving Walvis Ridge–Rio Grande Rise, a series of reconstructions for selected spreading anomaly times is shown in Figure 9. If a hot spot-generated seamount or ridge formed at a spreading-axis, it will be surrounded by spreading anomalies of the same age, which may on occasion be mapped onto the hot spot trail (Figure 2). Conversely, if hot spot magma erupts through older, previously formed seafloor, an age difference will be apparent between the age of the hot spot feature and that of the surrounding seafloor. The age data determined in this study therefore present an excellent opportunity to model the changing spatial relationship between the spreading-axis, the hot spot, and the evolving Walvis Ridge–Rio Grande Rise volcanic system, since anomaly 34 (84 Ma) time.

A suggested prerifting-rifting configuration of Africa, South America, the Parana–Etendeka flood basalts, and a postulated, large diameter hot spot, is shown in Figure 9*a*. From anomaly 34 time, spreading anomalies, which were forming at the time of each particular reconstruction, were rotated, along with the Walvis Ridge bathymetry (and African continent), to their respective predrift positions. An appropriate rotation parameter was calculated for each reconstruction from the Africa/hot spots finite poles given in Table 3. The corresponding anomaly picks on the South American plate, the Rio Grande Rise bathymetry

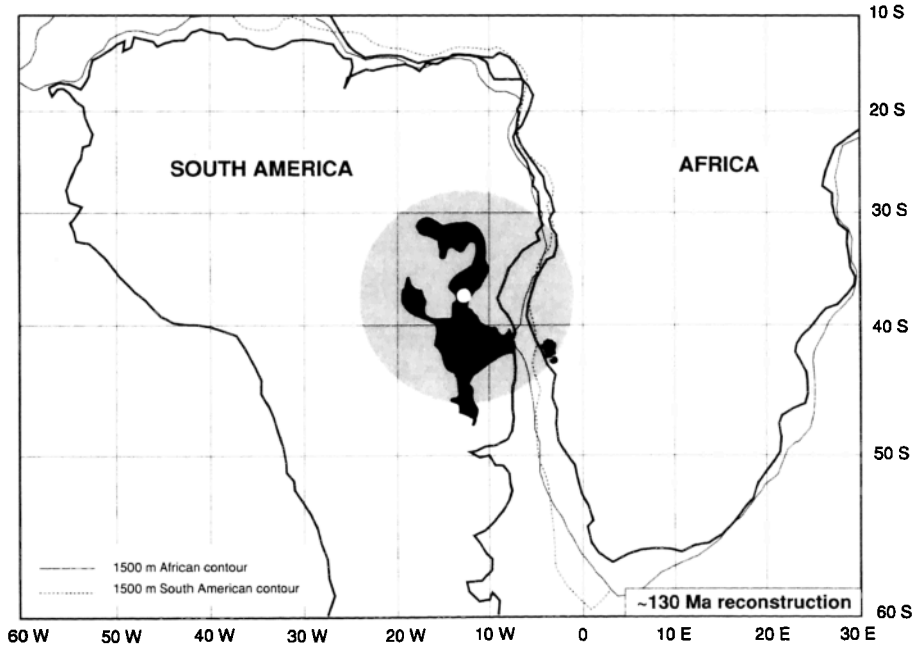

Fig. 9*a*. The shaded region represents a hypothesized, large-diameter hot spot, which formed above the upwelling Tristan plume (open circle) at ~130 Ma. A 130 Ma reconstruction parameter for Africa/hot spots motion was calculated such that the Etendeka flood basalts lie along the southeastern edge of this large diameter plume. The closure parameter of *Martin et al.* [1981], when combined with this 130 Ma Africa/hot spot rotation parameter, rejoins South America to Africa. Projection is centered on Tristan da Cunha.

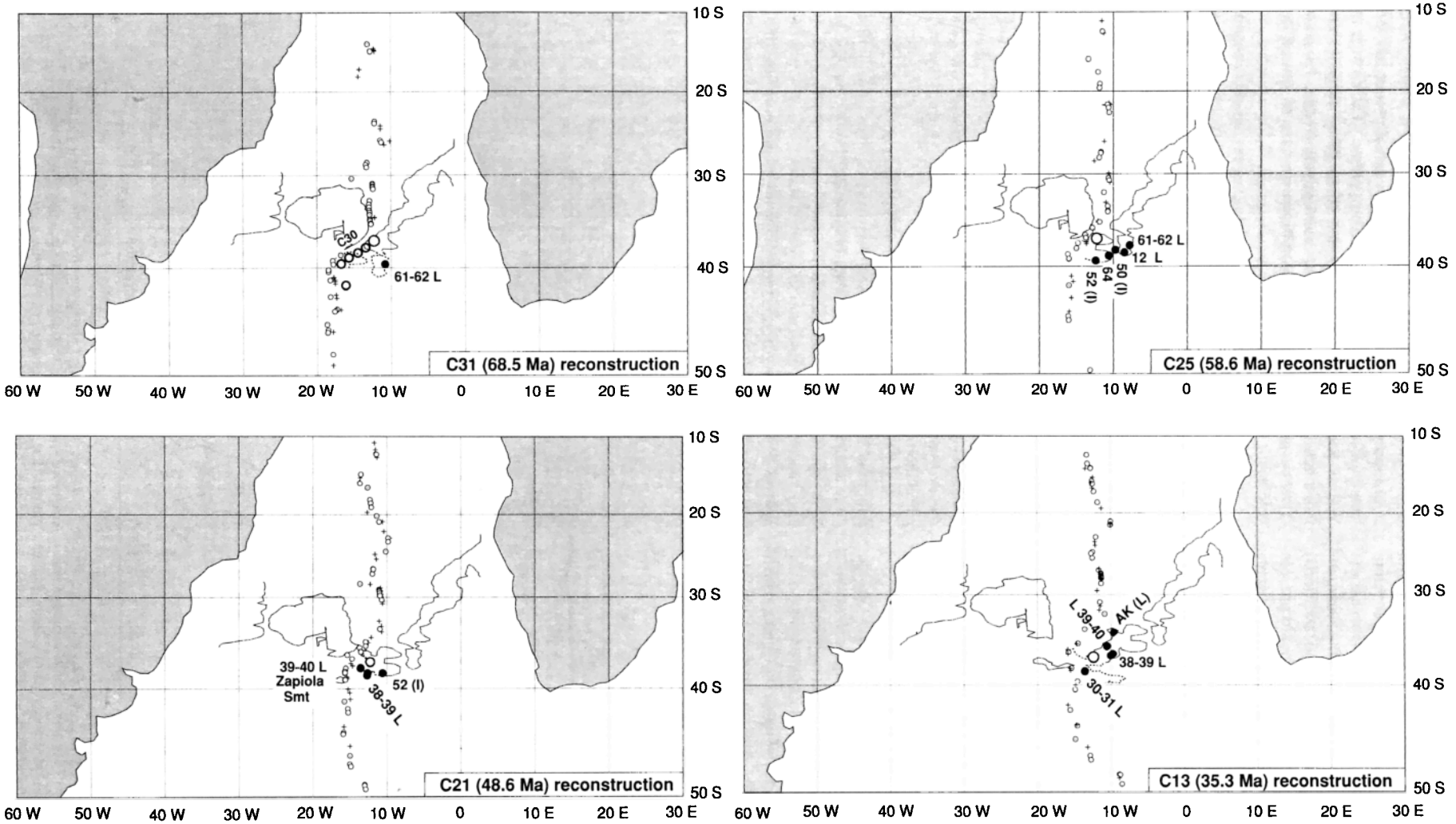

Fig. 9*b*. A series of reconstructions of the spatial relationship between the spreading-axis, the Tristan hot spot, and the evolving structure of the Walvis Ridge–Rio Grande Rise volcanic system is shown. The projections are centered on the island of Tristan da Cunha (shown as an open circle), i.e., the postulated center of the hot spot. For selected spreading anomaly times the configuration of seafloor spreading anomaly picks (corresponding to the age of the particular reconstruction), Walvis Ridge and Rio Grande Rise bathymetry, and the African and South American continents, have been reconstructed. An Africa/hot spots finite reconstruction pole was calculated for each reconstruction from the rotation parameters given in Table 3. A corresponding South America/hot spots rotation pole was calculated by the addition of a pertinent South America/Africa relative motion parameter [*Cande et al.*, 1988]. Magnetic anomaly picks are from Cande et al. [1988] with (pluses and small open circles) representing rotated African and South American anomaly picks, respectively. Bathymetry is from the DBDB 10 global bathymetry [National Geophysical Data Center, 1985]. Shaded portions of the Rio Grande Rise represent portions of this feature, which are considered to have formed at the time for which the reconstruction is shown. Dashed bathymetry indicates portions of the Walvis Rise–Rio Grande Rise system which had yet to evolve at the time of the particular reconstruction, and are shown for clarity. Basement ages for the Walvis Ridge–Rio Grande Rise are shown. The letters H, I, and L indicate whether a sample site is characterized by high, intermediate, or low Zr/Nb ratios, respectively, as defined in Figure 10. Mercator projection.

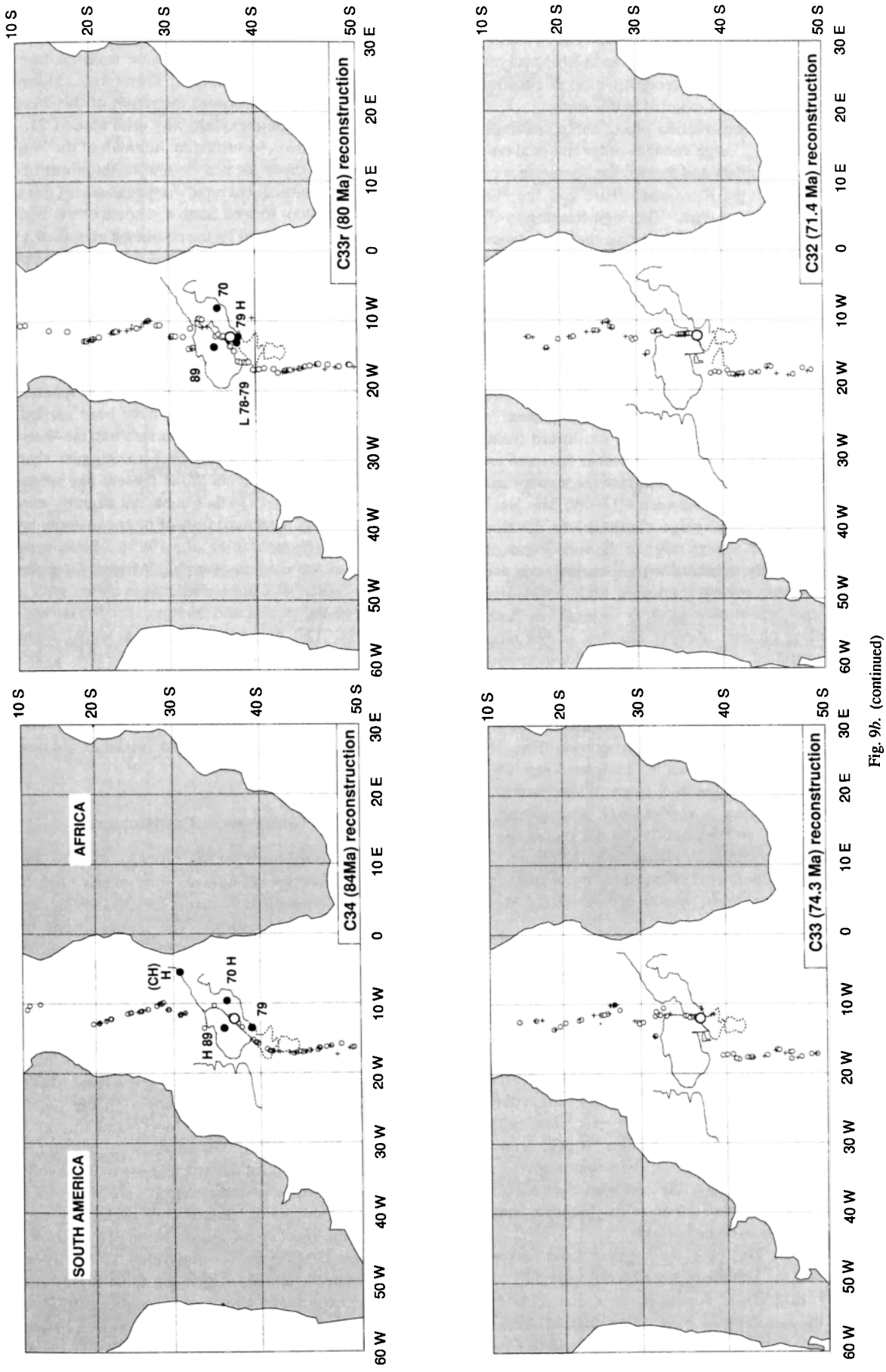

Fig. 9b. (continued)

(and the South American continent) were, in turn, rotated to their conjugate, predrift positions, by the addition of the appropriate South America/Africa relative motion [*Cande et al.*, 1988]. The extent to which the Walvis Ridge–Rio Grande Rise bathymetry had evolved at the time of each reconstruction is constrained primarily by the basement ages reported in this study.

The C34 (84 Ma) reconstruction places the spreading-axis astride the Tristan plume. Large volumes of hot material erupted along this divergent boundary and formed the conjugate western and eastern plateaus of the Rio Grande Rise and the Walvis Ridge, respectively (Figure 9*b*). The significant age-offset between seafloor located to the north versus that to the south of the Walvis Ridge (Figure 2) can be attributed to a prior history of easterly and southeasterly spreading-axis migrations beginning in Albian to late Aptian time, as discussed in an earlier section. The configuration of the spreading-axis, volcanic structure, and the hot spot in anomaly 34 time is strikingly similar to that which exists in present day Iceland.

At C33r (80 Ma) the northeastern shoulder of the Rio Grande Rise and the western edge of the Walvis Ridge plateau were formed. The narrow ridge which extends southward from the Walvis Ridge plateau, was constructed almost as far south as the 78-79 Ma DSDP transect, in conjunction with the western side of the Rio Grande Rise Plateau. Between C33r (80 Ma) and C32 (71.4 Ma) time, this narrow ridge continued to develop in conjunction with the N-S eastern ridge of the Rio Grande Rise. This N-S ridge apparently formed along a spreading-axis, which was continuously propagating southward and southeastward toward the hot spot, apparently in order to retain its position above the upwelling plume. Massive amounts of hot material must have been supplied to the spreading-axis by the plume in order for this massive lineament to have formed within such a relatively short time interval. As the spreading-axis propagated southward it invaded the previously formed seafloor which was in the process of migrating northward over the hot spot. Thus, while the South American plate may in fact have migrated in a NW-SE direction over the hot spot, the N-S ridge of the eastern Rio Grande Rise formed along a southwardly propagating, hot spot-fed spreading-axis, and apparently did not record the true direction of South American plate motion over the plume. As a result of this continued southward propagation, the asymmetry of the spreading-axis became most pronounced between C33r and C32 times.

By C31 (68.5 Ma), or earlier, the Walvis Ridge had commenced to bifurcate into three subparallel lineaments. The northern ridge formed on the spreading-axis, in conjunction with the southeastern terminus of the eastern Rio Grande Rise, while to the southeast a subparallel ridge was forming in an intraplate situation. Between C32 (71.4 Ma) and C30 (66.7 Ma) times a major spreading-axis jump occurred, which may have represented the final effort by the spreading-axis to regain its position over, or close to, the hot spot. Thus, by about C30 (66.7 Ma) time, or earlier, the northern side of the Walvis Ridge (and the southeastern portion of the Rio Grande Rise) was evolving as a plume-fed spreading-axis, while the southern portion of the Walvis Ridge was forming in an intraplate environment, as older seafloor began to migrate over the hot spot.

By about C21 (48.6 Ma) time, the hot spot could no longer sufficiently augment the volume of hot material upwelling along the westwardly migrating spreading-axis for continued construction of the Rio Grande Rise. The Zapiola seamount complex began to evolve about this time to the south of the Rio Grande Rise. The migration over the plume of the fracture zone, which represents the southern boundary of spreading-axis asymmetry (located to the north of Tristan da Cunha in Figure 2), may have switched the flow of plume material from the Rio Grande Rise to the Zapiola seamount region of the spreading-axis. The northward migration of this fracture zone, over the hot spot, could explain why until about C21 (48.6 Ma) the seafloor isochrons identified to the south of the Walvis Ridge were older than those located on and to the north of the ridge (Figure 2). The subsequent rapid disappearance of this age offset between the seafloor located north and south of the Walvis Ridge is therefore best explained by the combined effects of a westward migration of the spreading-axis away from the hot spot and an associated northward migration over the hot spot of the previously formed African lithosphere.

At C13 (35.3 Ma) the Zapiola Seamount complex ceased to evolve. A mirror image of the Zapiola Complex could have been formed on the African plate by the westward flow of plume material to the spreading-axis, beneath the lithosphere. If such a feature existed it would eventually have been carried over the Tristan plume and have been incorporated into the Walvis Ridge.

There is geochemical evidence to suggest that basaltic magmas, which have erupted at the present day spreading-axis, located due west of Tristan da Cunha, are slightly "enriched" by the continuation of westward flow of plume material beneath the African plate [*Humphris et al.*, 1985]. Such a continuous enrichment of the magmas forming African lithosphere at the latitude of Tristan da Cunha would have varied with increasing separation of the plume and the spreading-axis, which began about 70 Ma. This enriched geochemical signal, trapped in the African plate, might have been mixed into Walvis Ridge magmas, as this variable enriched African lithosphere migrated over the hot spot. Additional information about the history of hot spot and spreading-axis interactions is provided by a number of other approaches (e.g., geochemistry and isostasy) discussed in the following section.

Geochemical Compositions

Magmas derived from hot spots (ocean island basalts or OIB) and from seafloor spreading-axes (mid-ocean ridge basalts or MORB) are compositionally distinct, especially in certain trace element and isotopic ratios. The compositions of Walvis Ridge–Rio Grande Rise basalts vary in incompatible element abundances and ratios, rare earth elements (REE), and Sr, Nd, Pb isotopic ratios [*Humphris and Thompson*, 1982, 1983; *Richardson et al.*, 1982, 1984; *Thompson and Humphris*, 1984; *Thompson et al.*, 1983; *Humphris et al.*, 1985].

A decrease in the Zr/Nb ratio of the hot spot has occurred since the formation of the Etendeka-Parana flood basalts (Figure 10), which may be related to changes in the plate tectonic environment associated with the westward migration of the spreading-axis (Figure 9*b*). The elements Zr and Nb (and also Y and the REE elements) are of particular use in the investigation of magma source regions, as these elements are highly incompatible and their ratio will be influenced only slightly by variations in partial melting and crystal fractionation [*Erlank and Kable*, 1976; *Sun et al.*, 1979; *Pearce and Norry*, 1979]. They are also among the trace elements which are most highly resistant to mobilization by seawater alteration [*Thompson*, 1973].

High Zr/Nb ratios are evident in Etendeka-Parana, DSDP 516F (Rio Grande Rise plateau), CH 18 and CH 19, AII-93-21,

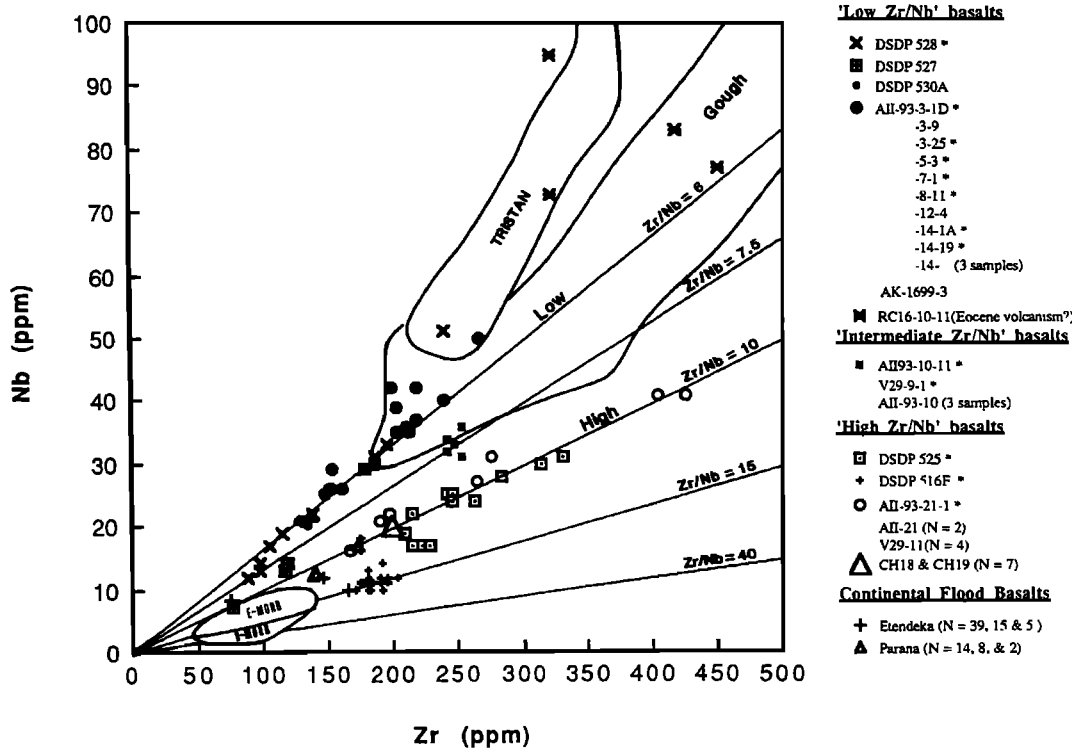

Fig. 10. Zr/Nb ratios for the Walvis Ridge–Rio Grande Rise hot spot system can be divided into "high", "intermediate", and "low" Zr/Nb basalts. "High" Zr/Nb basalts (apart from present-day spreading-axis basalts) are associated with continental flood and on-spreading-axis, hot spot volcanism. In contrast, "low" Zr/Nb ratios are associated with intraplate hot spot volcanism and hot spot-fed spreading-axis (i.e., DSDP 527, 528, and 530). Figure 9*b* illustrates this correlation between decreasing Zr/Nb ratios and the transition from on-spreading-axis to intraplate volcanism, within the Walvis Ridge–Rio Grande Rise system. Gough Island is a recently active volcano located to the southeast of Tristan da Cunha. Sources of data: Parana [*Fodor et al.*, 1985], Etendeka [*Marsh*, 1987], Walvis Ridge dredges [*Humphris and Thompson*, 1982, 1983], DSDP 530 and CH18 and 19 [*Humphris and Thompson*, 1983], DSDP 525A, 527 and 528 [*Thompson and Humphris*, 1984], DSDP 516F [*Thompson et al.*, 1983; *Weaver et al.*, 1983], Tristan da Cunha [*Weaver et al.*, 1987], Gough Island [*le Roex*, 1985; *Weaver et al.*, 1987], and MORB [*Humphris et al.*, 1985]. Asterisks denote samples for which ^{40}Ar-^{39}Ar ages have been determined. N = number of analyses for which a mean value has been determined.

V29-11 (eastern Walvis Ridge) and DSDP 525A (central Walvis Ridge) basalts (Figures 5 and 6). Apart from the flood basalts, these high Zr/Nb ratios may be characteristic of an on-axis situation (Figure 9*b*), as proposed by *Humphris et al.* [1985]. In such a tectonic environment large volumes of magma from the upper mantle MORB source region might have diluted the signal of the OIB source, as occurs at the main central rifting zone in Iceland [e.g., *Schilling et al.*, 1982, 1983]. The "enriched" and "depleted" MORB type recovered from the spreading-axis about ~550 km to the west of Tristan da Cunha [*Humphris et al.*, 1985] are the only known volcanic rocks in this region with higher Zr/Nb ratios.

A transition to low Zr/Nb ratios is first recorded within the Walvis Ridge–Rio Grande Rise system at DSDP sites 528 and 527 (79-80 Ma). However, low Zr/Nb basalts have been recovered from DSDP site 530, located about 20 km to the north of the Walvis Ridge (Figure 7), close to the African coast. Variations in ratios of Zr/Y or Y/Nb, with Zr/Nb, displayed by DSDP 530, 527, and 528 basalts, correspond well with predicted mixing curves calculated for depleted MORB and an enriched, Tristan-type end-member source, in contrast to DSDP 525A and dredged basalts [*Humphris and Thompson*, 1983]. This points to 527 and 528 basalts having formed at a hot spot-fed spreading ridge, as was the case for 530 basalts, which had formed at an earlier time [*Humphris and Thompson*, 1983]. A similar pattern of binary mixing between "enriched" (Tristan) and "depleted" (MORB) end-member sources is evident in spreading-axis basalts recovered due west of Tristan da Cunha. This indicates a continued sub-lithospheric connection between the Tristan hot spot and the spreading-axis [*Humphris et al.*, 1985]; however, earlier enrichment or fertilization of the upper mantle by the plume may also be of importance.

The remaining basalts recovered from the Walvis Ridge all exhibit low to intermediate Zr/Nb ratios, characteristic of their having erupted in an intraplate tectonic environment (Figure 9*b*). Basalts dredged from the Rio Grande Rise plateau (probably of Eocene age) exhibit low Zr/Nb ratios, in contrast with the underlying, on-axis, high Zr/Nb basement basalts (DSDP 516F) (Figure 9*b*).

Low Zr/Nb ratios for the island of Tristan da Cunha may result from the fact that, at very low degrees of partial melting, Zr does not behave as incompatibly as Nb; this could explain why the trend of the Tristan da Cunha Zr and Nb data intersects the Zr axis, rather than the origin [*Weaver et al.*, 1987]. Gough Island samples show a slight, but distinct decrease in Zr/Nb between the lower basalt series (about 1.0 Ma) and the upper basalt series (about 0.3 Ma) [*le Roex*, 1985], due possibly to the influence of decreasing degrees of partial melting.

Humphris and Thompson [1983] and *Humphris et al.* [1985], after *Chen and Frey* [1983], have suggested that as a transition to

an intraplate environment occurs, low degrees and low volumes of partial melting of the surrounding depleted lithosphere (i.e., previously formed African plate) will become important in determining the composition of the volcanic trail. Spreading-axis and hot spot interactions may therefore have controlled the mixing, and relative importance, of depleted MORB, enriched OIB, and low degrees and amounts of partial melts of the depleted lithosphere, thus indirectly determining the composition of Walvis Ridge and Rio Grande Rise basalts.

As a plume rises, however, it warms the surrounding mantle material by thermal diffusion, thus lowering its viscosity sufficiently to cause large-scale entrainment and mixing of asthenospheric source material [*Griffiths*, 1986]. The transition to less depleted magmas within the Reunion hot spot system (i.e., decreasing MORB component) is best explained by reduction in the entrainment of upper mantle material [*White et al.*, 1990]. Such a change in the extent of upper mantle entrainment may also have played a role in controlling the degree of enrichment of Walvis Ridge–Rio Grande Rise basalts. Sr, Nd, and Pb isotopic analyses are presently being conducted on available Walvis Ridge and Rio Grande Rise basalts, in order to determine the factors responsible for controlling temporal and spatial variations in composition [J. M. O'Connor et al., manuscript in preparation]. In conclusion, the change from high to low Zr/Nb ratios within the Walvis Ridge–Rio Grande Rise system broadly supports a model of transition from on-axis to intraplate volcanism.

ISOSTASY OF THE WALVIS RIDGE AND RIO GRANDE RISE

The transition from on-axis to intraplate hot spot volcanism within the Walvis Ridge–Rio Grande Rise system is supported by numerous gravity and geoid studies [*Detrick and Watts*, 1979; *Bulot et al.*, 1984; *Kogan et al.*,1985; *Gibert and Courtillot*, 1987; *Freedman*, 1987; *Diament and Goslin*, 1987]. The gravity signatures of aseismic ridges and seamounts are sensitive to the age (i.e., strength) of the lithosphere at the time of construction. Those features which formed in an intraplate setting (i.e., old, thick seafloor) are supported by the elastic stresses produced by the bending of the plate; as the plate distributes the compensating masses over a wide area, the gravity signature measured directly over the load will be large. In contrast, volcanoes which form on young lithosphere (i.e., near a spreading-axis) will be locally supported so that the compensating masses are located directly beneath the load; the resulting gravity anomaly measured above the feature will be small.

Gravity and geoid data measured over the Walvis Ridge and the Rio Grande Rise have been correlated with bathymetry in order to determine the mechanism by which they are isostatically compensated [*Detrick and Watts*, 1979; *Bulot et al.*, 1984; *Kogan et al.*, 1985; *Gibert and Courtillot*, 1987; *Diament and Goslin*, 1987]. *Detrick and Watts* [1979] have shown that from the African coast to about 3°E the Walvis Ridge is locally supported by an Airy-type thickening of the crust with a modeled crustal thickness in the range 15 km to 25 km. West of longitude 3°E, however, the Walvis Ridge is best explained by a plate model (i.e., a thin elastic plate overlying a weak fluid) with a modeled elastic thickness of between 5 and 8 km. These results are consistent with a transition from on-axis to intraplate hot spot volcanism on the Walvis Ridge at about 70 Ma.

The mechanical isostasy of the Walvis Ridge and the Rio Grande Rise has also been investigated by *Bulot et al.* [1984] using constraints imposed by SEASAT geoid data. In their study, the Walvis Ridge was divided into three overlapping subsections: an eastern (African coast to about 3°E), a central (about 3°E to about 0°), and a western section (about 0° to Tristan da Cunha). An Airy model calculated with a crustal thickness of 20 km is in good agreement with the experimental results obtained for both the eastern Walvis Ridge and the Rio Grande Rise. Experimental admittances using the plate model with an elastic thickness of 8 km and 6 km best fit the data from the central and western sections of the Walvis Ridge, respectively. This gradation in modeled plate thicknesses between the central and western study areas probably records the transition from on-axis to intraplate hot spot volcanism. *Diament and Goslin* [1987], however, have shown that the contributions of mechanical isostasy (off-axis formation) and density contrasts at depth (near-axis formation) are very different over adjoining domains along the Walvis Ridge. This can best be explained for the Walvis Ridge in terms of a rather complex history of hot spot spreading-axis interactions, as broadly documented in this study.

CHANGES IN SOUTH ATLANTIC OCEAN CIRCULATION

The transition from on-axis to intraplate hot spot volcanism within the Walvis Ridge–Rio Grande Rise may be indirectly recorded by an abrupt improvement in the oxidation state of South Atlantic bottom water at 55 to 58 Ma. *Liu* [1982], *Liu and Schmitt* [1984], *Wang et al.* [1986], *Liu et al.* [1988], and *Hu et al.* [1988] have proposed that under reducing conditions, Ce exists in seawater as a trivalent ion and is therefore incorporated along with the other trivalent rare earth elements (i.e., lanthanides) into seafloor sediments, by adsorption onto carbonate minerals. In contrast, under oxidizing conditions, Ce^{3+} is oxidized to Ce^{4+} and precipitates as very insoluble hydroxides. This results in depletion of Ce relative to the other trivalent rare earth elements in both seawater and sediments. Such Ce variations within marine carbonates represent a record of changes in palaeo-ocean bottom water redox conditions.

Carbonate sediment samples from DSDP 525A [*Liu*, 1982; *Liu and Schmitt*, 1984], DSDP 530A, B, located in ocean floor 20 km north of the eastern end of the Walvis Ridge [*Wang et al.*, 1986], and DSDP 516, 516F [*Hu et al.*, 1988] have been analyzed by the INAA technique in order to determine downcore Ce variations. All three sites show gradual Ce depletions (i.e. reducing seawater conditions) from the late Campanian (~80 Ma) until about 55 to 58 Ma, at which time an abrupt transition to present day Ce values (i.e., oxidizing seawater conditions) occurred. *Hu et al.* [1988] and *Liu et al.* [1988] have attributed such changes in oxidation state to improvements in the circulation of South Atlantic bottom water. Breaching of the Walvis Ridge–Rio Grande Rise barrier to bottom water circulation, as a result of the divergence of the spreading-axis and the hot spot, is a probable explanation for this improvement in circulation. Widening of the South Atlantic ocean basin and subsidence of the Romanche Fracture Zone (which acted as a barrier to deep bottom water flowing between the North and South Atlantic basins), may, however, have also played significant roles.

CONCLUSIONS

Volcanism within the Walvis Ridge–Rio Grande Rise volcanic system has been shown to be fundamentally age-progressive. The origin of the recently active island of Tristan da Cunha, the Walvis Ridge and Rio Grande Rise, and the Etendeka and Parana continental flood basalts, can therefore be attributed to a common source, the Tristan plume.

The Walvis Ridge and Rio Grande Rise formed in a synchronous, age-progressive fashion along a section of the South Atlantic spreading-axis, as the African and South American plates diverged apart, astride (or in close proximity to) the Tristan hot spot. Reconstructions of the spatial relationship between the spreading-axis, the hot spot, and the evolving Walvis Ridge–Rio Grande Rise system have shown that at about 70 Ma the spreading-axis migrated to the west, away from the hot spot. This westward migration of the spreading-axis was accompanied by a northward migration over the hot spot of previously formed seafloor. As a consequence, a transition from on-axis to intraplate hot spot volcanism occurred, which resulted in the termination of Rio Grande Rise formation. Support for this conclusion is provided by the fact that on-axis basalts have higher Zr/Nb ratios in comparison to those which erupted in an intraplate situation. Changes in the spatial relationship between the spreading-axis and the hot spot may have controlled the mixing, and relative importance of, depleted MORB, enriched OIB, and partial melts of the depleted ocean lithosphere. Isostasy studies also support a transition to intraplate volcanism on the Walvis Ridge beginning at about 70 Ma.

In the light of an improved understanding of the temporal-spatial evolution of the surface expression of the Tristan plume, i.e., the Walvis Ridge–Rio Grande Rise and associated continental flood basalt fields, rotation parameters for the motion of the African plate over the Tristan hot spot have been recalculated. These reconstruction poles predict a trail for the Tristan hot spot on the African plate which agrees with the distribution of ages along the Walvis Ridge. The N-S trending eastern ridge of the Rio Grande Rise formed, in all probability, along a hot spot-fed, southwardly propagating spreading-axis. This portion of the Rio Grande Rise apparently does not record the actual motion of the South American plate over the hot spot. Africa/hot spots rotation parameters were therefore not constrained to predict a trail which, on addition of South America/Africa relative motion poles, would follow the geometry of the N-S ridge of the Rio Grande Rise. Rather, the hot spot track cuts a NW-SE path across the Rio Grande Rise, following the NW-SE trending, elongated topography suggested for the rise from studies of the South Atlantic geoid. This result illustrates the critical importance of a detailed understanding of the evolution of individual hot spot systems such as the Walvis Ridge–Rio Grande Rise, in estimating reliable reconstruction poles.

The reconstructed motion of the African plate over hot spots has been extended to the North and South American plates by the addition of appropriate relative motion poles. The evolution of all significant hot spot systems on both of these plates has been discussed in detail. In order for the predicted track of the New England hot spot to pass through the region of the New England seamounts, the zero age location of this plume must be located in the vicinity of the central Atlantic spreading-axis at about 27°N. The existence of a prominent intermediate-wavelength geoid anomaly in this locality has been interpreted as supporting evidence for this conclusion. The Azores hot spot has been linked to the initiation of rifting, and consequent seafloor spreading, in the Rockall Trough.

Acknowledgments. The authors wish to thank Geoff Thompson who provided the dredge samples used in this study. Steve Cande generously provided magnetic anomaly data, and poles of relative motion in advance of publication. Brent Dalrymple and colleagues kindly provided the computer program used for the reduction of Ar-Ar data. One of us (J.O'C) wishes to acknowledge the advice and guidance of Lew Hogan during the analytical stages of this study. Suggestions by reviewer Steve Cande, an anonymous reviewer, associate editor Richard Gordon, and unofficial reviewer Gordon Ness, were both insightful and extremely helpful. Pierrick Roperch gave helpful advice on techniques in computer graphics. A map of Walvis Ridge bathymetry was provided by Jean Claude Sibuet. This work was supported primarily by the Office of Naval Research (grant N00014-87-K-0420).

REFERENCES

Almeida, F. F. M., Geologia e petrologia do argquipelago de Fernando do Noronha, *Monogr., 13*, Div. Geol. Min. Dep. Nac. Prod. Mineral., Rio de Janeiro, 1958.

Amaral, G., U. G. Cordani, K. Kawashita, and J. H. Reynolds, Potassium-argon dates of basaltic rocks from Southern Brazil, *Geochim. Cosmochim. Acta, 30*, 159-189, 1966.

Anderson, D. L., Hot spots, polar wander, Mesozoic convection and the geoid, *Nature, 297*, 391-393, 1982.

Aumento, F., Vesicularity of mid ocean pillow lavas, *Can. J. Earth Sci., 8*, 1315-1319, 1971.

Austin, J. A., Jr., and E. Uchupi, Continental-oceanic crustal transition off Southwest Africa, *Am. Assoc. Pet. Geol. Bull., 66*, 1328-1347, 1982.

Backman, J., R. A. Duncan et al., *Proc. Ocean Drill. Program, Initial Rep., 115*, 1085 pp., 1988.

Baker, B. H., and J. A. Miller, Geology and geochronology of the Seychelles Islands and structure of the floor of the Arabian Sea, *Nature, 199*, 346, 1963.

Baker, I., N. H. Gale, and J. Simons, Geochronology of the St. Helena volcanoes, *Nature, 215*, 1451-1454, 1967.

Barker, P. E., Tectonic evolution and subsidence history of the Rio Grande Rise, *Initial Rep. Deep Sea Drill. Proj., 72*, 953-976, 1984.

Barker, P. E., I. G. Gass, P. G. Harris, and R. W. LeMaitre, The volcanological report of the Royal Society expedition to Tristan da Cunha, *Philos. Trans. R. Soc. London., Ser. A, 256*, 439-578, 1964.

Blow, W. H., Deep Sea Drilling Project, Leg 3, Foraminifera from selected samples, *Initial Rep. Deep Sea Drill. Proj., 3*, 629-661, 1970.

Bolli, H. M., W. B. F. Ryan et al., Walvis Ridge-sites 362 and 363, *Initial Rep. Deep Sea Drill. Proj., 40*, 183-356, 1978.

Brereton, N. R., Corrections for interfering isotopes in the ^{40}Ar-^{39}Ar dating method, *Earth Planet. Sci. Lett., 8*, 427-433, 1970.

Bryan, W. B, and R. A. Duncan., Age and provenance of clastic horizons from hole 516F, *Initial Rep. Deep Sea Drill. Proj., 72*, 475-477, 1983.

Bukry, D., and M. N. Bramlette, Coccolith age determinations leg 3, Deep Sea Drilling Project, *Initial Rep. Deep Sea Drill. Proj., 3*, 589-612, 1970.

Bulot, A., M. Diament, M. G. Kogan, and J. Dubois, Isostasy of aseismic tectonic units in the South Atlantic Ocean and geodynamic implications, *Earth Planet. Sci. Lett., 70*, 346-354, 1984.

Cande, S. C., and P. D. Rabinowitz, Mesozoic sea floor spreading bordering conjugate continental margins of Angola and Brazil, *Proc. Annu. Offshore Technol. Conf., 3*, 1769-1776, 1978.

Cande, S. C., and P. D. Rabinowitz, Magnetic anomalies of the continental margin of Brazil, Offshore Brazil Map Ser, American Association of Petroleum Geologists, Tulsa, Okla., 1979.

Cande, S. C., J. L. LaBrecque, and W.B. Haxby, Plate kinematics of the South Atlantic: Chron 34 to present, *J. Geophys. Res., 93*, 13,479-13,492, 1988.

Cande, S. C., J. L. LaBrecque, R. L. Larson, W. C. Pitmann III, X. Golovchenko, and W. F. Haxby, *Magnetic Lineations of the World's Ocean Basins (map)*. Scale: approximately 1:27,400,000 at the equator, American Association of Petroleum Geologists, Tulsa, Okla., 1989.

Chaffey, D. J., R. A. Cliff, and B. M. Wilson, Characterization of the St. Helena magma source, edited by A. D. Saunders, and M. J. Norry, *Magmatism in the Ocean Basins*, Spec. Publ. 42, Geol. Soc. of London, pp. 257-276, 1989.

Chave, A. D., Lower Paleocene-upper Cretaceous magnetostratigraphy, sites 525, 527, 528, and 529, *Initial Rep. Deep Sea Drill. Proj., 74*, 525-532, 1984.

Chen, C.-Y., and F. A. Frey, Origin of Hawaiian tholeiite and alkalic basalt, *Nature, 302*, 785-789, 1983.

Cherkis, N. Z., H. S. Fleming, and J. M. Brozena, Bathymetry of the South Atlantic Ocean-3°S to 40°S, Map and Chart Ser. MCH-069, *Geol. Soc. of Am.*, Boulder, Colo., 1989.

Chevallier, L., and N. Vatin-Perignon, Volcanostructural evolution of Piton des Neiges, Reunion Island, Indian Ocean, *Bull. Volcanol., 45*, 287-298, 1982.

Ciesielski, P. F., Y. Kristoffersen et al., *Proc. Ocean Drill. Program, Initial Rep., 114*, 801 pp., 1988.

Clark, D. B., The Tertiary volcanic province of Baffin Bay, *Geol. Assoc. Can. Spec. Pap., 16*, 445-460, 1977.

Cordani, U. G., Idade do vulcanismo no Oceano Atlantico Sul, *Bol. Inst. Geocienc. Astron., Univ. Sao Paulo, 1*, 9-75, 1970.

Cordani, U. G., P. L. Sartori, and K. Kawashita, Geoquimica dos isotropes de estroncio e a evolucao da atividade vulcanica na Bacia do Parana, *An. Acad. Bras. Cienc., 52*, 811-818, 1980.

Cox, K. G., The role of mantle plumes in the development of continental drainage patterns, *Nature, 342*, 873-877, 1989.

Crough, S. T., Mesozoic hot spot epeirogeny in eastern North America, *Geology, 9*, 2-6, 1981.

Crough, S. T., W. J. Morgan, and R. B. Hargraves, Kimberlites: Their relation to mantle hot spots, *Earth Planet. Sci. Lett., 50*, 260-274, 1980.

Dalrymple, G. B., and D. A. Clague, Age of the Hawaiian-Emperor Bend, *Earth Planet. Sci. Lett., 31*, 317-321, 1976.

Dalrymple, G. B., and M. A. Lanphere, *Potassium Argon dating: Principles, Techniques, and Application to Geochronology*, W. H. Freeman, New York, 258 pp., 1969.

Dalrymple, G. B., and M. A. Lanphere, $^{40}Ar/^{39}Ar$ technique of K-Ar dating: A comparison with the conventional technique, *Earth Planet. Sci. Lett., 12*, 300-308, 1971.

Dalrymple, G. B., and J. G. Moore, Argon 40: Excess in submarine pillow basalts from Kilaueau Volcano, Hawaii, *Science, 161*, 1132-1135, 1968.

Dalrymple, G. B., E. C. Alexander, Jr., M. A. Lanphere, and G. P. Kraker, Irradiation of samples for $^{40}Ar/^{39}Ar$ dating using the Geological Survey TRIGA reactor, *U. S. Geol. Surv. Prof. Pap., 1176*, 1981*a*.

Dalrymple, G. B., M. A. Lanphere, and D. A. Clague, Conventional and $^{40}Ar/^{39}Ar$ ages of volcanic rocks from Ojin (site 430), Nintoku (site 432), and Suiko (site 433) seamounts and chronology of volcanic propagation along the Hawaiian-Emperor Chain, *Initial Rep. Deep Sea Drill. Proj., 55*, 659-676, 1981*b*.

Dalrymple, G. B., M. A. Lanphere, and M. S. Pringle, Correlation diagrams in $^{40}Ar/^{39}Ar$ dating: Is there a correct choice?, *Geophys. Res. Lett., 15*, 589-591, 1988.

Detrick, R. S, and A. B. Watts., An analysis of isostasy in the world's oceans: Three aseismic ridges, *J. Geophys. Res., 84*, 3637-3655, 1979.

Diament, M., and J. Goslin, Mechanical and thermal isostasy of submarine plateaus, (abstract), *Eos Trans. AGU, 68*, 1462, 1987.

Duncan, R. A., Hot-spots in the southern oceans-An absolute frame of reference for the motion of the Gondwana continents, *Tectonophysics, 74*, 29-42, 1981.

Duncan, R. A., Age progressive volcanism in the New England Seamounts and the opening of the central Atlantic Ocean, *J. Geophys. Res., 89*, 9980-9990, 1984.

Duncan, R. A., and R. B. Hargraves, ^{40}Ar-^{37}Ar geochronology of basement ages from the Mascarene Plateau, Chagos Bank, and the Maldives Ridges, *Proc. Ocean Drill. Program Sci. Results*, in press, 1990.

Dymond, J., Excess Ar in submarine pillow basalts, *Bull. Geol. Soc. Am., 181*, 1229-1232, 1970.

Emerick, C. M., and R. A. Duncan, Age progressive volcanism in the Comores Archipelago, western Indian Ocean and implications for Somali plate tectonics, *Earth Planet. Sci. Lett., 60*, 415-428, 1982.

Epp, D., and N. C. Smoot, Distribution of seamounts in the North Atlantic, *Nature, 337*, 254-257, 1989.

Erlank, A. J., and E. J. D. Kable, The significance of incompatible elements in Mid-Atlantic Ridge basalts from 45°N, with particular reference to Zr/Nb, *Contrib. Mineral. Petrol., 54*, 281-291, 1976.

Erlank, A. J., J. S. Marsh, A. R. Duncan, R. M. Miller, C. J. Hawkesworth, P. J. Betton, and D. C. Rex, Geochemistry and petrogenisis of the Etendeka volcanic rocks from SWA/Namibia, *Spec. Publ. Geol. Soc. S. Afr., 13*, 195-245, 1984.

Fleitout, L., C. Dalloubeix, and C. Moriceau, Small-wavelength geoid and topography anomalies in the South Atlantic Ocean: A clue to new hot spot tracks and lithospheric deformation, *Geophy. Res. Lett., 16*, 637-640, 1989.

Fodor, R. V., K. Keil, J. W. Husler, and E. H. McKee, Petrology and K-Ar age of volcanic tuff and ash from the Walvis Seamount Province, DSDP site 359, leg 39, Initial Rep. Deep Sea Drill., Proj., 39, 525-536, 1977.

Fodor, R. V., C. Corwin, and A. Rosinenberg, Petrology of Serra Geral (Parana) continental flood basalts, southern Brazil: Crustal contamination, source material, and South Atlantic magmatism, *Contrib. Mineral. Petrol., 91*, 54-65, 1985.

Foland, K. A., and H. Faul, Ages of the White Mountain Intrusives-New Hampshire, Vermont and Maine, U.S.A., *Am. J. Sci., 277*, 888-904, 1977.

Foland, K. A., L. A. Gilbert, C. A. Sebring, and J.-F. Chen, $^{40}Ar/^{39}Ar$ ages for plutons of the Monteregian Hills, Quebec: Evidence for a single episode of Cretaceous magmatism, *Geol. Soc. Amer. Bull., 97*, 966-974, 1986.

Foland, K. A., J.-F. Chen, L. A. Gilbert, and A. W. Hofmann, Nd and Sr isotopic signatures of Mesozoic plutons in northeastern North America, *Geology, 16*, 684-687, 1988.

Freedman, A. P., Marine geophysical applications of Seasat altimetry and the lithospheric structure of the South Atlantic Ocean, Ph.D. thesis, Mass. Inst. Technol., Cambridge, 1987.

Gartner, S., Coccolith age determinations leg 3, Deep Sea Drilling Project, *Initial Rep. Deep Sea Drill. Project, 3*, 613-627, 1970.

Gibert, D., and V. Courtillot, Seasat altimetry and the South Atlantic geoid, 1, Spectral analysis, *J. Geophys. Res., 92*, 6235-6248, 1987.

Gibert, D., V. Courtillot, and J.-L. Olivet, Seasat altimetry and the South Atlantic geoid, 2, Short-wavelength undulations, *J. Geophys. Res., 94*, 5545-5559, 1989.

Gilbert, L. A., and K. A. Foland, The Mont St. Hilaire plutonic complex: Occurrence of excess ^{40}Ar and short intrusion history, *Can. J. Earth Sci., 23*, 948-958, 1986.

Gillot, P.-Y., and P. Nativel, K-Ar chronology of the ultimate activity of Piton des Neiges, Reunion Island, Indian Ocean, *J. Volcanol. Geotherm. Res., 13*, 131-146, 1984.

Gillot, P.-Y., and P. Nativel, Eruptive history of Piton de la Fournaise volcano, Reunion Island, Indian Ocean, *J. Volcanol. Geotherm. Res., 36*, 53-65, 1989.

Griffiths, R. W., The differing effects of compositional and thermal buoyancies on the evolution of mantle diapirs, *Phys. Earth Planet. Inter., 43*, 261-273, 1986.

Guimaraes, I. P., A. N. Sial, and A. F. Silva Filho, Petrologia e geochimica da provincia alcalina Terciaria Fortaleza, Cera, An. *Congr. Bras. Geol.*, Salvador 2, XXXII, 577-588, 1982.

Hartnady, C. J. H., and A. P. le Roex, Southern Ocean hot spot tracks and the Cenozoic absolute motion of the African, Antarctic, and South American plates, *Earth Planet. Sci. Lett., 75*, 245-257, 1985.

Hawkesworth, C. J., M. S. M. P. N. Mantovani, P. N. Taylor, and Z. Palacz, Evidence from the Parana of south Brazil for a continental contribution to Dupal basalts, *Nature, 322*, 356-359, 1986.

Helgason, J., Shifts of the plate boundary in Iceland: Some aspects of Tertiary volcanism, *J. Geophys. Res., 90*, 10,084-10,092, 1985.

Herz, N., Timing of spreading in the South Atlantic: Information from Brazilian alkalic rocks, *Geol. Soc. Am. Bull., 88*, 101-112, 1977.

Hu, X., Y. L. Wang, and R. A. Schmitt, Geochemistry of sediments on the Rio Grande Rise and the redox evolution of the South Atlantic Ocean, *Geochim. Cosmochim. Acta., 52*, 201-207, 1988.

Humphris, S. E, and G. Thompson, A geochemical study of rocks from the Walvis Ridge, South Atlantic, *Chem. Geol., 36*, 253-274, 1982.

Humphris, S. E, and G. Thompson, Petrology and geochemistry of rocks from the Angola Basin adjacent to the Walvis Ridge: Deep Sea Drilling Project leg 75, site 530, *Initial Rep. Deep Sea Drill. Proj., 75*, 1099-1105, 1983.

Humphris, S. E., G. Thompson, J.-G. Schilling, and R. H. Kingsley, Petrological and geochemical variations along the mid-Atlantic Ridge between 46 S and 32 S; Influence of the Tristan da Cunha mantle plume, *Geochim. Cosmochim. Acta, 49*, 1445-1464, 1985.

Kent, D. V., and F. M. Gradstein, A Jurassic to recent chronology, in: *The Geology of North America: The Western North Atlantic Region, DNAG Ser.*, vol. M, edited by B. E. Tucholke and P. R. Vogt, pp. 45-50, Geological Society of America, Boulder, Colo., 1986.

Klitgord, K. D., and H. Schouten, Plate kinematics of the central Atlantic, in: *The Geology of North America: The Western North Atlantic Region, DNAG Ser.*, vol. M, edited by B. E. Tucholke and P. R. Vogt, pp. 351-378, Geological Society of America, Boulder, Colo., 1986.

Kogan, M. G., M. Diament, A. Bulot, and G. Balmino, Thermal isostasy in the South Atlantic Ocean from geoid anomalies, *Earth Planet. Sci. Lett., 74*, 280-290, 1985.

Kowsmann, R., R. Leyden, and O. Francisconi, Marine seismic

investigations, southern Brazil margin, *Bull. Am. Assoc. Pet. Geol.*, 546-557, 1977.

Kumar, N., Origin of "paired" aseismic rises: Ceara and Sierra Leone Rises in the equatorial, and the Rio Grande Rise and Walvis Ridge in the South Atlantic, *Mar. Geol., 30*, 175-191, 1979.

Kumar, N., and R. W. Embley, Evolution and origin of Cera Rise: An aseismic rise in the western equatorial Atlantic, *Geol. Soc. Am. Bull., 88*, 683-694, 1977.

Kumar, N., and L. A. P. Gamboa, Evolution of the Sao Paulo Plateau (southeastern Brazilian margin) and implications for the early history of the South Atlantic, *Geol. Soc. Am. Bull, 90*, 281-293, 1979.

LaBrecque, J. L.(Ed.) South Atlantic Ocean and adjacent continental margin *Reg. Atlas Ser., Atlas 13*, Ocean Drill. Program, College Station, Tex., 1986.

LaBrecque, J. L., J. Phillips, and J. A. Austin, The crustal age and tectonic fabric at the leg 73 sites, *Initial Rep. Deep Sea Drill. Proj., 73*, 791-798, 1984.

Ladd, J. W., South Atlantic sea floor spreading and Caribbean tectonics, Ph.D. thesis, 251 pp., Columbia Univ., New York, 1974.

Ladd, J. W., Relative motion of South America with respect to North America and Caribbean tectonics, *Geol. Soc. Am. Bull., 87*, 969-976, 1976.

le Roex, A. P., Geochemistry, mineralogy and magmatic evolution of the basaltic and trachytic lavas from Gough Island, South Atlantic, *J. Petrol., 26*, 149-186, 1985.

Leyden, R., H. Asmus, S. Zembruscki, and G. Bryan, South Atlantic diapir structures, *Am. Assoc. Pet. Geol. Bull., 60*, 196-212, 1976.

Liu, Y.-G., Chemical element profiles by instrumental neutron activation analysis 2, Representative sediment and basalt samples taken from DSDP 678 m core, site 525A, leg 74, Walvis Ridge, M.S. thesis, Oregon State Univ., Corvallis, 1982.

Liu, Y.-G., and R. A. Schmitt, Chemical profiles in sediment and basalt samples from deep sea drilling project leg 74, hole 525A, Walvis Ridge, *Initial Rep. Deep Sea Drill. Proj., 74*, 713-730, 1984.

Liu, Y.-G., M. R. U. Miah, and R. A. Schmitt, Cerium: A chemical tracer for paleo-oceanic redox conditions, *Geochim Cosmochim Acta, 52*, 1361-1371, 1988.

MacIntyre, R. M., A. P. Dickin, A. E. Fallick, and A. N. Halliday, An isotopic and geochronological study of the younger igneous rocks of the Seychelles, *Eos Trans. AGU, 66*, 1137, 1985.

Manivit, M., Paleogene and upper Cretaceous nannofossils from Deep Sea Drilling Project, leg 74, *Initial Rep. Deep Sea Drill. Proj., 74*, 475-499, 1984.

Marsh, J. S., Basalt geochemistry and tectonic discrimination within continental flood basalt provinces, *J. Volcanol. Geotherm. Res., 32*, 35-49, 1987.

Martin., A. K., C. J. H. Hartnady, and S. Goodlad, A revised fit of South America and South Central Africa, *Earth Planet. Sci. Lett., 54*, 293-305, 1981.

Mascle, J., and J. D. Phillips, Magnetic quiet zones in the South Atlantic, *Nature, 240*, 80-84, 1972.

McDougall, I., The geochronology and evolution of the young volcanic island of Reunion (Indian Ocean), *Geochim. Cosmochim. Acta, 35*, 261-288, 1971.

McDougall, I., and R.A. Duncan, Age progressive volcanism in the Tasmantid Seamounts, *Earth Planet. Sci. Lett., 89*, 207-220, 1988

McDougall, I., and T. M. Harrison, *Geochronology and Thermochronology by the $^{40}Ar/^{39}Ar$ Method*, 212 pp., Oxford University Press, New York, 1988.

McDougall, I., and C. D. Ollier, Apparent K-Ar ages from Tristan da Cunha, South Atlantic, *Geol. Mag., 119*, 87-93, 1982.

McDougall, I., and N. R. Ruegg, Potassium-argon dates on the Serra Geral formation of South America, *Geochim. Cosmochim. Acta, 30*, 191-195, 1966.

Melfi, A. J., Potassium-argon ages for core samples from Southern Brazil, *Geochim. Cosmochim. Acta, 31*, 1079, 1967.

Melson, W. G., and G. Thompson, Glassy abyssal basalts, Atlantic sea floor near St. Pauls Rocks: Petrography and composition of secondary clay minerals, *Bull. Geol. Soc. Am., 84*, 703-716, 1973.

Molnar, P., and J. Stock, Relative motions of hot spots in the Pacific, Atlantic and Indian Oceans since late Cretaceous time, *Nature, 327*, 587-591, 1987.

Morgan, W. J., Convection plumes in the lower mantle, *Nature, 230*, 42-43, 1971.

Morgan, W. J., Deep mantle convection: Plumes and plate motions, *Am. Assoc. Pet. Geol Bull , 56*, 203-213, 1972.

Morgan, W. J., Hot-spot tracks and the opening of the Atlantic and Indian Oceans, in The Sea, vol. 7, pp. 443-488, Wiley Interscience, New York, 1981.

Morgan, W. J., Hot-spot tracks and the early rifting of the Atlantic, *Tectonophysics, 94*, 123-139, 1983.

Musset, A. E. and P. F. Barker, $^{40}Ar/^{39}Ar$ age spectra of basalts, Deep Sea Drilling Project site 516, *Initial Rep. Deep Sea Drill. Proj., 72*, 467-470, 1983.

National Geophysical Data Center, Worldwide gridded bathymetry, DBDB10, *Announc. 85-MGG-01*, Boulder, Colo., 1985.

Needham, H. D., D. Carre and J. C. Sibuet, Bathymetrie de la Ride de Walvis et du Bassin du Cap, Ocean Atlantique Sud, report, Dep. Geosci. Mar., Inst. Franc. de Rech. pour l'Exploitation de la Mer, Orleans, France, 1986.

Neill, W. M., Possible continental rifting in Brazil and Angola related to the opening of the South Atlantic, *Nature Phys. Sci., 245*, 104-107, 1973.

O'Connor, J. M., On the trail of South Atlantic hot spots: Implications for reconstructing African and South American plate motions (abstract), *Eos Trans. AGU, 70*, 1135, 1989.

Pearce, J. A., and M. J. Norry, Petrogenetic implications of Ti, Zr, Y and Nb variations in volcanic rocks, *Contrib. Mineral. Petrol., 69*, 33-47, 1979.

Ponte, F. C., and H. E. Asmus, The Brazilian marginal basins: Current state of knowledge, *An. Acad. Bras. Cienc, 48* (suppl.), 215-239, 1976.

Rabinowitz, P. D., Geophysical study of the continental margin of southern Africa, *Geol. Soc. Am. Bull., 87*, 1643-1653, 1976.

Rabinowitz, P. D., Geophysical study of the continental margin of southern Africa, Reply, *Geol. Soc. Am. Bull., 89*, 793-796, 1978.

Rabinowitz, P. D., and J. L. LaBrecque, The Mesozoic South Atlantic Ocean and evolution of its continental margins, *J. Geophys. Res., 84*, 5973-6002, 1979.

Richards, M. A., R. A. Duncan, and V. E. Courtillot, Flood basalts and hot-spot tracks: Plume heads and tails, *Science, 246*, 103-107, 1989.

Richardson, S. H., A. J. Erlank, A. R. Duncan, and D. L. Reid, Correlated Nd, Sr and Pb isotope variations in Walvis Ridge basalts and implications for the evolution of their mantle source, *Earth Planet. Sci. Lett., 59*, 327-342, 1982.

Richardson, S. H., A. J. Erlank, D. L. Reid and A. R. Duncan, Major and trace element and Nd and Sr isotope geochemistry of basalts from the DSDP leg 74 Walvis Ridge transect, *Initial Rep. Deep Sea Drill. Proj., 74*, 739-754, 1984.

Saemundsson, K., Outline of the geology of Iceland, *Joekull, 29*, 7-28, 1979.

Samson, S. D., and E. C. Alexander, Jr., Calibration of the interlaboratory ^{40}Ar-^{39}Ar dating standard, Mmhb-1, *Chem. Geol., 66*, 27-34, 1987.

Schilling, J.-G., Geochemical and isotopic variation along the Mid-Atlantic Ridge axis from 79°N to 0°N, in The Geology of North America, The Western North Atlantic Region, DNAG Ser., vol. M, edited by B. E. Tucholke and P. R. Vogt, pp. 137-156, Geological Society of America, Boulder, Colo., 137-156, 1986.

Schilling, J.-G., R. H. Kingsley, and J. G. DeVine, Galapagos hot spreading center system: Spatial, petrological and geochemical variations 83°W-101°W, *J. Geophys. Res., 87*, 5593-5610, 1982.

Schilling, J.-G., M. Zajac, R. Evans, T. Johnston, W. White, J. D. Devine, and R. Kingsley, Petrologic and geochemical variations along the Mid-Atlantic Ridge from 29°N to 73°N, *Am. J. Sci., 283*, 510-586, 1983.

Schlanger, S. O., M. O. Garcia, B. H. Keating, J. J. Naughton, W. W. Sager, J. A. Haggerty, J. A. Philpotts, and R. A. Duncan, Geology and geochronology of the Line Islands, *J. Geophys. Res., 89*, 11, 261-11, 272, 1984.

Sclater, J. G., and D. P. McKenzie, Palaeobathymetry of the South Atlantic, *Geol. Soc. Am. Bull., 84*, 3203-3216, 1973.

Scrutton, R. A., Geophysical study of the continental margin of southern Africa-Discussion, *Geol. Soc. Am. Bull., 89*, 791-793, 1978.

Seidemann, D., Effects of submarine alteration on K-Ar dating of deep-sea igneous rocks, *Geol. Soc. Am. Bull., 88*, 1660-1666, 1977.

Seidemann, D., $^{40}Ar/^{39}Ar$ studies of deep-sea igneous rocks, *Geochim. Cosmochim. Acta, 42*, 1721-1734, 1978.

Sibuet, J.-C., and J. Mascle, Plate kinematic implications of Atlantic equatorial fracture zone trends, *J. Geophys. Res., 83*, 3401-3421, 1978.

Sibuet, J.-C., W. W. Hay, A. Prunier, L. Montadert, K. Hinz, and J.

Fritsch, Early evolution of South Atlantic: Role of the rifting phase, *Initial Rep. Deep Sea Drill. Proj., 75*, 469-481, 1984.

Siedner, G., and J. A. Miller, K-Ar age determinations on basaltic rocks from south-west Africa and their bearing on continental drift, *Earth Planet. Sci. Lett., 4*, 451-458, 1968.

Siedner, G., and J. G. Mitchell, Episodic mesozoic volcanism in Namibia and Brazil: A K-Ar isochron study bearing on the opening of the South Atlantic, *Earth Planet. Sci. Lett., 30*, 292-302, 1976.

Srivastava, S. P., and C. R. Tapscott, Plate kinematics of the North Atlantic, in The Geology of North America: The western North Atlantic Region, DNAG Ser., vol. M, edited by B. E. Tucholke and P. R. Vogt, 379-404, Geological Society of America, Boulder, Colo., 1986.

Stock, J. M., and P. Molnar, Some geometrical aspects of uncertainties in combined plate reconstructions, *Geology, 11*, 697-701, 1983.

Sullivan, K. D., and C. E. Keen, Newfoundland Seamounts: Petrology and geochemistry, *Geol. Assoc. Can. Spec. Pap., 16*, 461-476, 1977.

Sun, S. S., R. W. Nesbitt, and A. Y. Sharaskin, Geochemical characteristics of mid-ocean ridge basalts, *Earth Planet. Sci. Lett., 44*, 119-138, 1979.

Svisero, D. P., H. O. A. Meyer, and H. Tsai, Kimberlites in Brazil: An initial report, in *Kimberlites Diatremes, and Diamonds: Their Geology, Petrology and Geochemistry*, edited by H. O. A. Meyer, and F. R. Boyd, pp. 92-100, AGU, Washington, D. C., 1979.

Taras, B. D., and S. R. Hart, Geochemical evolution of the New England Seamount chain: Isotopic and trace element constraints, *Chem. Geol., 64*, 35-54, 1987.

Thompson, G., A geochemical study of the low temperature interaction of seawater and oceanic igneous rocks, *Eos Trans. AGU, 54*, 1015-1019, 1973.

Thompson, G., and S. E. Humphris, Petrology and geochemistry of rocks from the Walvis Ridge: Deep Sea Drilling Project leg 74, sites 525, 527, and 528, *Initial Rep. Deep Sea Drill. Proj., 74*, 755-764, 1984.

Thompson, G., S. Humphris, and J.-G. Schilling, Petrology and geochemistry of basaltic rocks from the Rio Grande Rise, South Atlantic: Deep Sea Drilling Project, leg 72, hole 516, *Initial Rep. Deep Sea Drill. Proj., 72*, 457-466, 1983.

Tucholke, B. E., and N. C. Smoot, Evidence for age and evolution of Corner Seamounts and Great Meteor seamount chain from multibeam bathymetry, *J. Geophys. Res.*, in press, 1990.

Turner, G., and P. H. Cadogan, Possible effects of ^{39}Ar recoil in ^{40}Ar-^{39}Ar dating of lunar, *Proc. Lunar Sci. Conf., 5*, 1601-1615, 1974.

Vandoros, P., and M. A. F. Oliveira, Sobre o fonolito de Messejana, Ceara, *An. Acad. Bras. Cienco., 40*, 203-206, 1968.

Vogt, P. R., and G. L. Johnson, Transform faults and longitudinal flow beneath the mid-ocean ridge, *J. Geophys. Res., 80*, 1399-1428, 1975.

Vogt, P. R., B. Zondek, P. W. Fell, N. Z. Cherkis, and R. K. Perry, Seasat altimetry, the North Atlantic geoid, and evaluation by shipborne subsatellite profiles, *J. Geophys. Res., 89*, 9885-9903, 1984.

Walker, D. A., and I. McDougall, $^{40}Ar/^{39}Ar$ and K-Ar dating of altered glassy volcanic rocks: The Dabi Volcanics, P.N.G., *Geochem. Cosmochim. Acta., 46*, 2181-2190, 1982.

Wang, Y. L., Y.-G. Liu, and R. A. Schmitt, Rare earth element geochemistry of south Atlantic deep sea sediments: Ce anomaly change at ≈ 54 My, *Geochim. Cosmochim. Acta, 50*, 1337-1355, 1986.

Weaver, B. L., N. G. Marsh, and J. Tarney, Trace element geochemistry of basaltic rocks recovered at site 516, Rio Grande rise, *Initial Rep. Deep Sea Drill. Proj., 72*, 451-455, 1983.

Weaver, B. L., D. A. Wood, J. Tarney, and J. L. Joron, Geochemistry of ocean island basalts from the South Atlantic: Ascension, Bouvet, St. Helena, Gough, and Tristan da Cunha, Alkaline Igneous Rocks, edited by J. G. Fitton, and B. G. J. Upton, *Spec. Publ. 30*, pp. 253-267, Geol. Soc. of London, 1987.

Weiss, W., Upper Cretaceous foraminiferal biostratigraphy from the Rio Grande Rise: Site 516 of leg 72, *Initial Rep. Deep Sea Drill. Proj., 72*, 715-721, 1983.

Wendt, I., H. Kreuser, P. Muller, U. von Rad, and H. Raschke, K-Ar ages of basalt from Great Meteor and Josephine seamounts (eastern North Atlantic), *Deep Sea Res., 23*, 849-862, 1976.

White, R., and D. McKenzie, Magmatism at rift zones: The generation of volcanic continental margins and flood basalts, *J. Geophys. Res., 94*, 7685-7729, 1989.

White, W. M., M. M. Cheatham, and R. A. Duncan, Isotope geochemistry of leg 115 basalts and inferences on the history of the Reunion mantle plume, in *Proc. Ocean Drill. Program Sci. Results*, in press, 1990.

Wilson, J. T., A possible origin of the Hawaiian Islands, *Can. J. Phys., 41*, 863-870, 1963.

York, D., Least squares fitting of a straight line with correlated errors, *Earth Planet. Sci. Lett., 5*, 320-324, 1969.

J. M. O'Connor and R. A. Duncan, College of Oceanography, Oregon State University, Corvallis, OR 97331.

(Received March 14, 1989;
revised March 14, 1990;
accepted March 22, 1990.)